Individuality across environmental context in *Drosophila melanogaster*

Thomas F. Mathejczyk, Cara Knief, Muhammad A. Haidar, Florian Freitag, Tydings McClary, Mathias F. Wernet* and Gerit A. Linneweber*

Institut für Biologie

Abteilung Neurobiologie

Fachbereich Biologie, Chemie und Pharmazie

Freie Universität Berlin

*: corresponding authors

Contact: mathias.wernet@fu-berlin.de

Gerit.linneweber@fu-berlin.de

Abstract

Over the past decade, several studies have demonstrated that idiosyncratic animal behaviors remain stable over long time periods. The stability of individually variable behaviors over time is often referred to as an animal's individuality, or personality. However, most experimental studies have focused on individuality in a single, well-defined environmental context, whereas it is well-established from population studies that animal behavior is highly context-dependent. The 'person-situation debate' in humans and decades of observations of animal individuality under intrinsically variable natural conditions raise the question of whether and to what extent animal behavior remains stable across different situations, such as changing environmental contexts. For instance, one individual might be generally more visually guided than another, or rely only on one particular visual cue, or even on this very cue only in a specific environmental context. Here, we use a combination of both well-established and novel behavioral assays to demonstrate the relationship between individual behavior and variable environmental context under tightly controlled laboratory conditions in the model system *Drosophila melanogaster*. The stability of three individual traits (termed exploration, attention, and anxiety) was investigated under changing environmental contexts (temperature, visual cues, arena shape), in both walking and flying flies. We find that individuality is highly context-dependent, but even under the most extreme environmental alterations tested, stability of behavior always persisted in at least one of the traits. Furthermore, our quantification reveals a hierarchical order of environmental features influencing individuality. In summary, our work demonstrates that, similar to humans, fly individuality persists across different contexts, and individual differences shape behavior across variable environments, thereby making the underlying developmental and functional mechanisms amenable to genetic dissection.

Introduction

Animal species display enormous interindividual differences in behavior. The temporal stability of these interindividual differences allows for defining these idiosyncrasies as animal individuality, also called animal temperament, behavioral syndrome, or even personality [1-4]. Animal individuality has been described for numerous species and behaviors, including: mouse exploration behavior [5], great tit feeding preferences [6], octopus threat and feeding behavior [7], pea aphid threat responses [8], as well as vinegar fly handedness [9,10], olfaction [11], phototaxis [12], and object orientation [13]. The temporal stability of individuality allows for discriminating it from short-term behavioral changes, like internal state variations. Furthermore, temporal stability of behavior allows modifications by learning [14] and behavior-based natural selection [15]. Historically, the 'nature vs. nurture' debate (i.e., genome vs. environment) has shaped our understanding of the origins of behavioral individuality [16]. Stochastic developmental processes are a more recently found factor [13,17], providing an additional layer to gene-environmental interactions [18]. Most experimental studies on animal individuality have focused on a single behavior set in a singular environment, yet commonly used definitions of animal individuality in predominantly field-based disciplines such as behavioral ecology [3], and the definition of human personality entails behavioral stability across situations [19]. Similar to humans, animals will never re-encounter the exact same situation under natural conditions, and individuality can be an important factor in determining the ecological success of an animal and, as a consequence, its entire population [20]. It is, therefore, crucial to understand how an animal's individuality interacts with variable environments. Despite decades of interest in animal individuality across situations, the experimental evidence remains insufficient, and the results are contradictory, with studies arguing for [21-24] and against [25,26] individuality across situations with many finding mixed results [27-29]. Here we sought to systematically investigate the stability of individual behavioral differences across situations using laboratory-controlled variable environmental conditions.

There is ample evidence for the stability of human personality and animal individuality over time [30,31]. Intuitively, humans attribute stable personalities to other humans [32]. The stability

of human behavior across situations, including environmental context, nevertheless remains highly debated, with several studies arguing for [30,33] and against it [19,34]. Summarized as the 'person-situation debate', psychologists have argued for over a century about the relationship between personality and the situational environment, placing this question at the core of personality psychology [19]. Animal models for behavioral stability across situations provide an opportunity to address this question. In our study, the situation is the sum of all environmental features where a specific behavioral task is performed. The work presented here establishes a quantitative animal model to investigate this and related questions about behavioral stability across environmental situations.

The vinegar fly *Drosophila melanogaster* provides an enormous toolset for studying individuality and its origins across multiple scales, from neurons to circuits, to behavior. This comprises a rapidly unfolding connectome [35,36], an extensive collection of cell type-specific, binary expression systems [37,38], and a similarly extensive collection of tools for manipulating neuronal function, including neuronal silencers [39,40], activators [41], and thermogenetic [42] and optogenetic [43,44] effectors. Hence, the availability of tools and reagents for manipulating small, defined sets of neurons is no longer a major limitation in answering questions about individual behavioral differences. Instead, what has been missing is an integrative approach combining different high-throughput behavioral assays, which would allow for behavioral screening and classification of large quantities of individual flies for several different behavioral parameters across a variety of environmental contexts.

In recent years, mainly low-throughput, single-fly visual assays like the classical two-stripe Buridan assay [45,46], arenas for tethered walking [47] or virtual flight [48] have been used to study behavioral individuality in vison-based tasks [13,49]. In Buridan's paradigm, flies walk between two inaccessible visual targets (two vertical high-contrast stripes). The stripes are presented in a homogenously illuminated surrounding with no other visual or non-visual cues. Apart from work on individuality involving Dorsal Cluster Neurons (DCNs) [50], also known as Lobula Columnar Neuron 14 (LC14) [51], Buridan's paradigm has been used to show the importance of the central complex for normal walking speed [52] and for studying photoreceptor

108 function or development [53,54], and visual memory [55]. Other circular arenas have been frequently
109 used to study locomotory activity without visual stimuli [56-58].

110 In contrast to these low throughput assays, high throughput assays for studying the
111 behavioral responses of large amounts of animals have been used primarily for genetic
112 screens. Examples include apparatuses to study phototaxis [59], geotaxis [60], olfactory learning
113 [61,62], and circadian rhythms [63]. The Ethoscope [64] and MARGO [65] are recent additions to this
114 repertoire that offer several additional high-throughput assays. Except for the *Drosophila*
115 activity monitors (DAM, Trikinetiks), Ethoscope, and MARGO, these group assays cannot
116 distinguish individual behavioral differences. Only the Ethoscope and MARGO provide some
117 visual modules. Hence, progress towards understanding individuality in visually guided
118 behaviors in a high-throughput fashion remains meager, with few exceptions [9,10,12].

119 To investigate the influence of the environment on the stability of visually guided
120 individuality and, to systematically quantify individuality across many behavioral traits and their
121 dependency on the environment in walking flies, we built a new multi-parameter assay called
122 Indytrax. Indytrax is a compact and affordable Mathworks MATLAB-based modular assay and
123 tracker for high-throughput individual ethological quantification. The assay includes swappable
124 modules for multiple high-throughput Buridan paradigms, a Y-maze choice assay for studying
125 the decision-making and locomotor handedness [10], and a simple setup to quantify locomotor
126 activity in large groups of flies [57]. We used this tracker to determine the relative contribution of
127 various environmental features (temperature, visual cues, arena shape) to the stability of
128 individual behavior. Our results show that identically defined visual stimuli (stripe color, width,
129 and length) do not necessarily evoke the same behavior in an individual when presented in
130 different environments. Conversely, we find that specific individual behavioral traits (attention,
131 exploration, and anxiety, categorized via multiple behavioral parameters) remain stable even
132 in different environments. Finally, using an LED-based virtual flight arena, we show that
133 attention towards a stimulus remains stable even across different modalities of locomotion
134 (walking versus flying) when using the same Buridan-type visual stimulus. Hence, we find
135 stable behavioral traits across situations in our fly model, in analogy to what has been

demonstrated for humans [30,33]. Altogether, our results provide the foundation for understanding the complex interaction between individuality and the environment, including the question of why individual behavior is more unpredictable in variable naturalistic conditions, much like the stability across situations in human subjects [19].

140 **Materials and Methods**

141 Animals

142 All experiments were performed using one week old wild-type *Drosophila melanogaster*
143 (CantonS (Source: Bassem Hassan) and TopBanana [66]) reared on a standard *Drosophila*
144 yeast cornmeal medium (7.5g Agar, 64g cornmeal, 160g yeast, 85.5ml sugar cane syrup in 1L
145 of water) at 25°C and 50% relative humidity under a 12/12 light/dark rhythm. Individual flies
146 were placed into the behavioral arenas using a fine brush and were allowed to accommodate
147 for about 10 minutes before any experiment. The behavioral arenas and flies were cooled on
148 ice for Y-maze experiments before gently loading single flies into the chambers using a fine
149 brush. For experiments with clipped wings, the wings were clipped close to the hinge under
150 CO_2 anesthesia, and flies were tested after being allowed to recover within individual vials for
151 at least two days.

152

153 **Setups**

154 **Setup 1: Standard Buridan Arena**

155 Assay

156 Two Buridan setups were used: type A uses fluorescent tubes for background
157 illumination (as described in [13,67]). Type B utilizes a panoramical LED matrix (RGB, 384x128
158 pixels, pixel size 0.9°, 120Hz frame rate, 5kHz refresh rate, < 1ms Pixel update latency), which
159 is easily addressable via HDMI for stimulus presentation (see Fig. 1a). For a detailed
160 description of the assays and tracking procedures, see supplemental Fig. S1. Flies were
161 walking on a circular platform (diameter 12cm) between two opposing black vertical stripes
162 (angular extent 12° horizontal and 90° vertical measured from the center of the platform). A
163 trench of water surrounded the platform to prevent the flies from escaping (type A) or a clear
164 plastic hemispherical dome coated with Sigmacote (Sigma-Aldrich, SL2-25ML) from the inside
165 (type B). Single-fly walking behavior was recorded at 25°C and 50% relative humidity for 15
166 minutes (450x450, 8-bit greyscale, 20 Hz, AVI, Mjpeg compression, 90% quality). Before
167 changing an experimental condition, flies were placed back into single vials for recovery.

168

169 Automated tracking procedure

170 Data was analyzed either in real-time using previously described code (type A, see [67])
171 or offline using a custom-written MATLAB code (type B, available for download from
172 github.com/LinneweberLab/individuality-assays, see supplemental Fig. S1c), respectively.
173 Thresholded video frames and overlaying trajectories are displayed continuously in a separate
174 window to allow the experimenter to assess tracking quality. The MATLAB code works as
175 follows: the circular region of interest (ROI) is automatically detected based on adaptive
176 thresholding and subsequent filtering of the thresholded ROI based on area. Once the ROI is
177 detected, a background image is generated by calculating the maximum intensity between a
178 recorded video's first and last frames. All flies that moved between those frames will not appear
179 in this background-only image. During tracking, the background image is subtracted from each
180 consecutive frame to simplify the thresholding of the fly. For each frame, the centroid of these
181 thresholded pixels is stored. Should more than one object be detected within a ROI (e.g.,
182 through pixel noise), the x-/y-coordinates of the object closest to the fly's position in the
183 previous frame are stored. If a fly is lost, the tracker keeps the last known position of the fly
184 until it is detected again.

185

186 Data output

187 Once tracking is completed, the raw tracking results are converted to real-world units
188 (mm) and saved into a .mat-file. Before further analysis, minimal movements are filtered out
189 by only updating the fly's position if a certain walking threshold (0.8mm/frame) is detected. For
190 each fly, a figure can be saved, allowing for a quick overview of the walking trajectory, and a
191 variety of behavioral parameters are also saved into a separate .txt-file to simplify further data
192 analysis. For a detailed explanation of calculated parameters, see supplemental table 1. For
193 an in-depth analysis of Buridan data, sophisticated data analysis routines describing many
194 behavioral parameters were previously developed [67]. To simplify data integration and

compatibility, the raw trajectories can also be saved to a pair of .TXT and .DAT files which can later be read and analyzed by previously available software [67].

Setup 2: IndyTrax multi-arena platform

Assay

To allow for high-throughput behavioral quantification under various tightly controlled environmental contexts, we designed the novel assay system IndyTrax. In short: single flies are transferred to an array of small behavioral arenas. They are filmed from below against near-infrared (850nm + Lee filters 87C IR-pass filter on camera objective) LED illumination (Fig. 3). Compared to published Buridan assays [67], this allows tracking flies in the absence of visible light, but also has the advantage that flies cannot see the camera lens which might otherwise appear as a high-contrast object from within the arena. The assay was designed to allow for the tracking of flies in various possible arena shapes and numbers. We created three different 3D-printable arena types (supplemental Fig. S4e-g), which can be downloaded from github.com/LinneweberLab/individuality-assays. For individuality analysis, we used the multi-Buridan and Y-maze arenas. The setup was built from commercially available and 3D-printed parts. For a part list, see the supplemental table 2. All 3D-printed parts and behavioral assays were printed on a Prusa i3 mk3 printer using black or white PLA filament (Verbatim 55318) and can be downloaded from github.com/LinneweberLab/individuality-assays. Similarly, the MATLAB code tracking and data analysis can be downloaded from there. For detailed instructions on how to install and run the code, see supplemental information. With a computer running MATLAB already available, we estimate the building cost for a complete, temperature- and humidity-controlled enclosure, including all behavioral assays, at about 3500€.

Temperature- and humidity-controlled enclosure

Behavioral arenas are located within a black climate-controlled metal enclosure. Temperature and humidity within the enclosure can be regulated using two 3D-printed

223 humidifiers and a heating plate (see supplemental Fig. S4a). Ambient temperature and
224 humidity can be set at any desired value using this configuration and kept stable over a long
225 time (see supplemental Fig. S4c). Since small enclosed arenas are prone to heat build-up, we
226 placed all temperature- and humidity-sensors within the center arena (arena 13) for Buridan
227 experiments and close to the flies in Y-maze experiments. For Buridan experiments, this limits
228 the number of simultaneously trackable arenas to 24 but allows more accurate climate control
229 within the chambers.
230
231 Small-scale Buridan-stimuli arrays
232 We modified the basic design of previously published behavioral arenas optimized for
233 Buridan object orientation behavior [67] by implementing changes in four major areas to allow
234 for high throughput tracking: Firstly, we reduced the arena diameter to allow for filming an array
235 (5x5) of optically isolated Buridan arenas with only a single camera (Fig. 3). Secondly, flies are
236 walking on circular translucent acrylic plates (49mm diameter) which allows for filming flies
237 from below against infrared back-illumination, hence avoiding problems with dead angles that
238 would arise when filming cylindrical arrays from above. Thirdly, during experiments, flies are
239 contained on their respective acrylic platform by clear hemispherical plastic domes (Fig. 3b).
240 This removes the necessity of cutting the flies' wings before experiments and saves space by
241 making the water-filled moats of the original design superfluous. Plastic domes were coated
242 with Sigmacote (Sigma-Aldrich, SL2-25ML) from the inside to prevent the flies from sitting on
243 the dome surface. Fourthly, to provide a scalable, homogeneously illuminated white
244 background for optical stimulus presentation, the fluorescent tubes of the original design were
245 replaced with electroluminescent (el-)foil wrapped around translucent acrylic cylinders (Fig.
246 3b). Such el-foils can be cut to size and have low heat emission. They emit light evenly over
247 the whole surface, minimizing unwanted intensity cues within the arenas. El foils are driven at
248 2 kHz, thus providing virtually flicker-free white illumination to the flies. For creating the Buridan
249 object orientation stimulus, thin black stripes (12° wide as measured from the arena center)
250 were 3D printed and glued vertically to the inside of the arena walls 180° apart, thereby creating

251 high-contrast objects against a uniform white background (Fig. 3b). Individual arenas were
252 fitted into a 5x5 array. Every other arena within the array was rotated by 90° counter-clockwise
253 to increase the robustness of behavioral readouts by canceling out possible directional artifacts
254 created within the enclosure.
255
256 Walking behavior was recorded at 50% relative humidity for 15 minutes (1200x1200
257 pixel, 8-bit greyscale, 15 Hz, AVI, Mjpeg compression, 90% quality) with either the el-foil-
258 illumination on, in darkness, at 23°C or 32°C, respectively. After being tested in the Buridan
259 assay, the flies were put back into single vials overnight to allow for recovery before testing
260 them in the Y-maze assay the next day around the same time.
261
262 Y-maze array
263 We constructed a modular 3D-printable Y-maze array (144 arenas, 300x300x2mm)
264 based on a previously published design [65]. The Y-maze plates were placed between two
265 320x320x3mm borosilicate glass plates. The bottom side of the upper glass plate was coated
266 three times using Sigmacote (Sigma-Aldrich, SL2-25ML) to prevent the flies from walking on
267 the upper plate (Fig. 3c). Directly below the arenas and above the upper glass plate, we placed
268 a layer of white paper (Evercopy premium 80g, Ref. 1902C) for light diffusion and to restrict
269 the view of the flies outside of the arenas. For individuality experiments, we covered the outer
270 arenas with black tape and tracked flies only within 100 arenas located in the center. This
271 made keeping track of individual fly identities easier when switching between the different
272 behavioral assays. Videos of walking flies were recorded at 50% relative humidity for 30
273 minutes (1200x1200 pixel, 8-bit greyscale, 15 Hz, AVI, Mjpeg compression, 90% quality) under
274 white light illumination, in darkness, at 23°C or 32°C, respectively. For white light illumination,
275 we placed a 30x30cm LED panel (Tween Light 30 x 30 cm LED panel, 4000k, 16W) on top of
276 the arenas and temporarily removed the infrared-pass filter from the camera objective. Y-maze
277 experiments were all done consecutively on the same day (light on 23°C, light off 23°C, light
278 on 32°C, light off 32°C).

Automated tracking procedure

We developed a fully-automated MATLAB-based tracking code that allows users to adjust parameters like arena number and size and generates output data for all videos within a user-selectable folder. The code assumes only one fly per region of interest. This saves processing time and increases tracking robustness by not having to match multiple fly identities between frames. Before running the code, the experimenter must create a camera calibration file using the MATLAB camera calibration toolbox (see supplemental information). This allows for more accurate tracking results by correcting lens distortions (supplemental Fig. S4d). If the camera stays immobile, this procedure must be done only once, usually only a few minutes. As long as the arenas filmed are arranged in rows and columns, the code can handle virtually any shape or number of arenas, making it ideal for tracking flies across different behavioral assays (supplemental Fig. S4e-g). Regions of interest (ROIs) are detected based on adaptive thresholding and subsequent filtering of thresholded ROI-objects based on the area (supplemental Fig. S4e-g, middle). Once the ROIs are detected and sorted, a background-subtracted image is generated, allowing the user to determine a detection threshold, above which all pixels will be interpreted as foreground objects (supplemental Fig. S4e, third from left). During tracking, background subtraction and object thresholding is performed for each frame, and for each ROI the centroid of the thresholded fly is extracted and saved. Thresholded pixels and trajectories are displayed continuously in a separate window to allow the experimenter to assess tracking quality. If more than one object is detected within a ROI (e.g. through pixel noise), the x-/y-coordinates of the object closest to the fly's position in the previous frame is stored. If a fly is lost, the tracker keeps the last known position of the fly until it is detected again. The average tracking speed for 24 ROIs/flies was about 20hz with MATLAB running on an Intel i5 3Ghz CPU. For tracking 400 ROIs/flies average tracking speed was about 5hz.

Data output

307 Data output is the same as described for our standard Buridan arenas.

308

309 **Setup 3: Virtual flight simulator**

310 Assay

311 We designed a novel, easy-to-assemble, and easy-to-use virtual flight simulator using
312 affordable 3D-printable and off-the-shelf parts (Fig. 5a-c) to quantify behavioral responses
313 during flight. For a detailed description of the setup and custom code, see supplemental Fig.
314 S9. In short, using a tethering station (for description, see [48]), flies were cooled down for
315 immobilization and glued to a steel pin (0.1mm diameter, 10mm length, www.entosphinx.cz)
316 using UV-cured glue (Bondic). Once tethered, single flies were put between two neodymium
317 magnets (magneto-tether; upper magnet: diameter 5mm, lower magnet: ring, outer diameter
318 10mm, inner diameter 5mm). Once the appropriate distance between the magnet is found
319 (about 20mm), the magnetic field allows the flies to rotate freely around their yaw-axis while
320 keeping the steel pin in place (Fig. 5b). The tip of the steel pin is inserted into a V-shaped
321 sapphire bearing (1mm diameter) to reduce friction. For re-initiation of flight, air puffs can be
322 delivered from below via a membrane pump. A panoramic LED matrix surrounding the
323 magneto-tether was used for Buridan stimulus presentation (RGB, 256x128 pixels, 120Hz
324 frame rate, 5kHz refresh rate, pixel size 1.4°, angular extent 360° horizontal x 100° vertical,
325 stripe width: 12°). The LED matrix controller is connected to a computer via HDMI, allowing an
326 easy and flexible stimulus creation and presentation (Novastar mctrl 660 pro, 120Hz, < 1ms
327 Pixel update latency). Flies were filmed from below under near-infrared illumination (Fig. 5c),
328 and each fly's heading was tracked in real-time (90 Hz) using a custom-written MATLAB code
329 (available for download from github.com/LinneweberLab/individuality-assays). Before starting
330 the experiment, each fly was tested for 120s with an optomotor stimulus (rotating stripe pattern,
331 120°/s, 40x CW and 40x CCW, respectively) to assess the flies' ability to rotate smoothly (Fig.
332 5d, left). After this, flies were presented with the Buridan stimulus with varying contrast (100%,
333 50%, 100% inverted; stripe width 30°), and their heading was tracked for 3x4 min. Flies were
334 then carefully separated from the steel pin and transferred into single vials for overnight

recovery before being re-tethered and tested the following day around the same time. For flight vs. walking experiments, flies were tested for 10 min while flying under a 100% contrast Buridan stimulus (stripe width 12° from a fly's perspective) before being gently separated from the steel pin and being transferred into the LED Buridan assay (Type B), where they were tested for 15min under a 100% contrast Buridan stimulus (stripe width 12° from a fly's perspective).

Automated tracking procedure

The code for tracking a fly's heading in 360° can be downloaded from github.com/LinneweberLab/individuality-assays. Flight tracking is done in real-time at 90fps (see supplemental Fig. S9c). A timestamp is created for each incoming camera frame, and two different thresholded images are computed with different Gaussian filter settings. A strong filter setting blurs out the legs of the fly and allows for thresholding only the fly's body and calculating a heading angle between 0° and 180° through ellipse fitting. By subtracting the thresholded body pixels from a weaker filtered version of the same frame, the limbs and wings (visible when the fly stops flying) can also be tracked separately if the experimenter wants. To calculate the heading between 0° and 360°, the centroid of thresholded body pixels is set to (0,0) within a fictive coordinate system (see supplemental Fig. S9c), and the body axis is aligned with the x-axis. The head region is assigned based on the sum of pixels within the 4 axis quadrants (smallest area of either I+IV or II+III, respectively). Once the heading is calculated, it is stored together with the original video frame for additional offline data analysis, if desired. When a fly stops flying (wings get detected in the video), a command is sent to a connected Arduino, which controls a relay to switch on a membrane pump and provide an air puff to reinitiate flight. During tracking, the thresholded video is displayed together with the computed heading to allow the experimenter to assess tracking quality.

Data output

After tracking, raw heading data, a graphical overview image, and a table containing computed behavioral parameters are saved automatically for each fly which can be used for further data analysis. For a detailed explanation of all calculated parameters, see supplemental table 1.

Data analysis

All data analysis was performed with MATLAB. For angular calculations, we used algorithm presented in [68]. After a test for normality (Shapiro-Wilk-Test), behavioral data between groups was compared using the paired T-test. For correlating individual data, we calculated Pearson correlation coefficients. For walking data, an arena's center region (edge-corrected area) was defined as the circular area around the center with a radius of 80% of the arena radius. The maximum color value (red) for generating heatmaps was set to the 95%-quantile of the count distribution to increase data visibility.

377 **Results**

378 The goal of our study was to understand to what extent animal individuality is influenced
379 by situational changes in the environment, i.e., how much of an animal's individuality remains
380 after one or more environmental features change. Based on our previous work on animal
381 individuality [13], we started our analysis in the multiparametric two-stripe Buridan's paradigm
382 (Fig. 1a, supplemental Fig. S1 for technical details) [13,67]. As expected, we measured
383 interindividually variable, yet remarkably stable behavioral responses, both on the individual
384 (Fig. 1b, Fig. 2a, supplemental Fig. S3a) and mean group level (supplemental Fig. S2a), when
385 tested in the exact same situation with all environmental features kept the same. This was true
386 for the five representative behavioral parameters (out of 20 parameters total, see supplemental
387 Table T1 and supplemental Fig. S8), defined as falling into three behavioral traits: exploration
388 (% of time walked, walking speed), attention (vector strength, angular velocity), and anxiety
389 (centrophobicity).

390 Modifying the visual stimulus within the Buridan arena (0, 1, and 2 stripes were tested,
391 Fig. 1c, Fig. 2b, and supplemental Fig. S2b and S3b) significantly affected the mean group
392 behavior across all three behavioral traits (supplemental Fig. S2b). Especially the population
393 means of three parameters (% of time walked, vector strength, and centrophobicity) were
394 strongly affected by the stimulus modification. Surprisingly, despite this change in population
395 means, we observed only a minor effect on individuality (Fig. 1c and Fig. 2b, measured by a
396 high Pearson correlation coefficient and a consistent rank within the distribution). The
397 individuality for the traits exploration and anxiety persisted even upon modulation (variation of
398 stripe number) and after removing visual cues from the arena. Only those parameters
399 describing the fly's attention towards visual cues showed an unsurprising reduction in
400 behavioral stability upon removal of the visual stimuli (Fig. 2b). Altogether, these results
401 demonstrate that individuality persisted after stimulus modifications within the same arena,
402 even when the modifications resulted in altered population responses.

403 To further characterize the surprising relationship between individuality and population
404 means upon situational changes, we modified the homogeneity of background illumination in

405 the Buridan arena using two different diffuser materials (paper and acryl-based covers of
406 fluorescent ring lights) and compared these conditions to a newly designed Buridan LED arena
407 displaying the same visual stimulus (stripes of the same color, width, and height) (Fig. 1d, Fig.
408 2c and supplemental Fig. S2c and S3c). We measured no significant differences between the
409 population means of the two diffuser conditions and only minor group-based changes
410 compared to the LED Buridan (supplemental Fig. S2c). We then tested the correlation of
411 individual behavior across these conditions, as a measurement of behavioral stability,
412 expecting high correlations. Indeed, the different diffusers within the same arenas only had
413 minor effects on the behavior of individual flies (Fig. 1d). Conversely, the individual response
414 changed dramatically when the same fly was tested again in the LED arena (Fig. 1d). A fly's
415 attention and anxiety parameters quantified within the original arena did not allow for any
416 prediction for the LED arena (Fig. 2c). Significant correlations between the LED arena and the
417 original arenas were only measured for exploration parameters (Fig. 2c). This unpredictability
418 of individual fly behavior across situations was once again particularly surprising since group-
419 based performances remained similar (supplemental Fig. S2c). Finally, a detailed comparison
420 of males and females revealed only quantitative but no qualitative differences across all
421 parameters between the two sexes (supplemental Fig. S2 and supplemental Fig. S3).

422 Based on the surprising result that individuality [1] of visual orientation behavior is more
423 strongly influenced by the arena type (despite producing very similar population responses)
424 and, only to a lesser degree, dependent on the visual cue (despite strong differences in the
425 population response), we set out to characterize the contribution of environmental situations
426 to individuality even more quantitatively. We therefore built a multiplatform high-throughput
427 assay (Indytrax) to quantitatively study the behavior of the same individual flies in different
428 environmental situations (Fig. 3, technical details supplemental Fig. S4).

429 Using Indytrax, we compared the behavioral parameters of each fly in eight different
430 environmental situations (Fig. 4, supplemental Fig. S6, S7, S8). The flies were tested in two
431 independent arenas (Buridan and Y-maze) at two different temperatures (23°C and 32°C,
432 supplemental Fig. S5) and under both light and dark conditions. Our analysis showed that

433 temperature significantly affected exploration parameters on the population mean level. As
434 expected, most animals tested were more explorative at higher than at lower temperatures
435 (reviewed in: [69]) (supplemental Fig. S6). Despite these population changes, individuals kept
436 their rank within the population independent of the changed baseline activity. For example, fly
437 #1 was the least explorative, fly #2 exploration performance ranked medium, and fly #3 the
438 highest (Fig. 4a). The graphical analysis of exploration parameters (Fig. 4b) confirmed that
439 most individuals maintain their rank in the distribution under different temperatures and light-
440 dark conditions, whereas the individual distribution rank changed between the different arena
441 types. This relationship was less pronounced for attention parameters. The detailed correlative
442 analysis between individuals underscores these observations (Fig. 4c and supplemental Fig.
443 S7 and full analysis supplemental Fig. S8): Amongst the exploration parameters, the
444 percentage of time walked significantly correlated between individuals (Pearson r=0.263-
445 0.398) independently of temperature, illumination, and arena. Walking speed was highly
446 correlated between individuals (Pearson r=0.81, 0.825) under temperature and illumination
447 changes but uncorrelated in different arena types (Pearson r=0.091). Vector strength was the
448 most correlated attention parameter. The individual correlations ranged from Pearson r=0.533
449 to -0197. Angular velocity significantly correlated for temperature and illumination (Pearson
450 r=0.246, 0.354) but not in different arenas (Pearson r=0.087). The same is true for anxiety
451 measured through centrophobicity (Pearson r=0.694, 0.740, 0.033). In summary, these data
452 revealed that individuality measured as three traits is mostly unaffected by temperature and
453 illumination but strongly affected by the arena type. Our analysis confirmed that even in
454 situations with a large effect on the mean group behavior (like temperature), individual
455 behavioral stability of idiosyncrasies remained high, while conversely, other environmental
456 situations like the arena type had little impact on the mean but a rather massive effect on
457 individual behavioral stability (Fig. S6). Qualitatively similar results leading to the same
458 conclusions were obtained for both sexes (Fig. S6a, S7a) and two different genotypes (Fig.
459 S6b, S7b)

460 Next, we drastically modified the behavioral situation while keeping the visual stimulus
461 as constant as possible. We, therefore, decided to investigate the influence of a fly's modality
462 of locomotion (walking versus flying) on individuality. To do this, we designed a new virtual
463 flight arena for tethered flight utilizing the exact same LED panels as were used in the LED
464 Buridan arena (Fig. 5a-c and supplemental S9 for technical details), to maximize the similarity
465 of the visual context. This flight simulator tracked a fly's heading in real-time in response to
466 dynamic or static panoramic visual stimuli with high resolution (1.4° pixel size). This allowed
467 us to quantitatively compare the visual decisions of both walking and flying flies in response to
468 standard optomotor and Buridan-like stimuli (Fig. 5d-e). We first tested individuality in flying
469 flies over time under the same and a set of modified visual stimuli (Fig. 6, supplemental Fig.
470 S10 and S11). Each fly was tested over two consecutive days under three different visual
471 conditions (dark stripes on a bright background with either 50% or 100% contrast, and an
472 inverted Buridan with bright stripes on a dark background and 100% contrast) (Fig. 6a).
473 Overall, the flies showed some individuality in visual attention across days and contrast. This
474 was also true for the inverted Buridan stimulus, in which the flies oriented themselves toward
475 the dark areas, similar to previous results [70]. To allow a quantitative comparison across
476 behavioral traits between walking and flight behavior, we derived an adapted set of parameters
477 for exploration and attention quantification (exploration parameters: # of pauses, Absolute
478 angular velocity; attention parameters: Vector strength, Angular velocity, and Median heading
479 axial, Fig. 6b). The resulting analyses revealed individuality in flying flies (Fig. 6c). Only the
480 inversion of the Buridan stimulus resulted in variable angles towards the black background on
481 different days. However, it is remarkable that on a given day, each fly selected an arbitrary
482 heading that was kept for the entire experimental length (Fig. 6a). Again, the quantitative
483 analysis between males and females did not reveal qualitative differences (Fig. S11).
484 After confirming that individuality also existed in flying flies, we tested how different
485 locomotion modalities affected a given animal's behavioral individuality. Behavioral parameters
486 of both walking and flying flies were quantified in response to the same panoramic LED screen
487 displaying an identical two-stripe Buridan stimulus (Fig. 7a, supplemental Fig. S12 and S13).

488 We expected one of three possible outcomes: 1. There is no stability of individual behavioral
489 traits across flying and walking, 2. Only some behavioral traits are similar across flying and
490 walking. 3. The fly's individuality remains stable across the same visual cue, independent of
491 the locomotive modality. Subsequent quantitative analysis indeed revealed a significant
492 correlation for angular velocity between flying and walking flies (Fig. 7b), indicating that a fly's
493 attention is, to some degree, preserved independent of the locomotor modality. In contrast, we
494 found no statistically significant correlations for any of the exploration parameters between
495 flying and walking. Finally, a more detailed analysis revealed mostly comparable results for
496 male and female data (supplemental Fig. S12 and S13).

497 In summary, the data presented here reveal a hierarchical influence of different
498 parameters within the environmental context on individuality (Fig. 8): First, we conclude that
499 time (at least within the frame of days) has a negligible influence on individual behavioral
500 responses (the basis of the definition of animal individuality in a single situation), since we
501 found stability of individual behavioral traits and parameters over time in both locomotor
502 modalities, walking and flying. Second, temperature had the second weakest impact on
503 individuality (although only tested for walking behavior). This contrasts the dramatically altered
504 population mean responses, a difference that can be explained by scaled individual responses
505 in which individuals keep the rank in the population. Third, the nature of the visual input
506 appears to influence the individual orientation responses but has little impact on the exploration
507 parameters. Finally, we identified the most critical situational environmental features that
508 determine individual responses as both the arena type and the locomotor modality (walking
509 vs. flying). Therefore, we conclude that the individuality of visually guided behaviors persists
510 specifically in some traits across situations, but the environmental context plays a prominent
511 role in defining individual behavioral responses.
512

Discussion

Our work presented here focused on the question of whether the combination of stable behavioral parameters ranging across different traits and therefore defining an animal's individuality are invariable across situations or whether they are re-shaped by different environmental contexts. This question is closely related to the questions in the human 'person-situation debate' [19]. Until now, in the neurosciences individuality across situations has been largely ignored since, the commonly used definition of animal individuality only refers to the repeatability of behavior over time in a single environmental situation [1]. The contrary is true for mainly field and observation-based sciences such as ethology and behavioral ecology that have since decades acquired observations for [28,29] or against [25,26] behavioral stability across situations, with some of the most convincing work probably found in hermit crabs [21,22], blue tits [23], and geese [24]. Our work establishes animal individuality across situations under several tightly controlled laboratory conditions, revealing that animal individuality shares remarkable similarities to what has been described in human personality research. In agreement with Vansteelandt, 2004 our results are in line with the concept of the personality triad, emphasizing the interplay of individual, situation, and behavior (in humans: person, situation, and behavior) [71].

Our results confirm that under the same environmental situation and stimulus, animals produce interindividually variable, but extremely stable behavioral responses when being retested [72]. Therefore, stable and individually variable behaviors likely result from individual brain properties that persist over long timescales (in this paper days as shown in previous papers months [13]), contrasting unstable random behavioral variations like sudden internal state variations. Hence, when presented with the same stimulus in the same situation, each individual responds variably but repetitively so, pointing towards a deterministic and hardwired basis of individual properties [10,13].

The variability of the situational environmental context makes individual animal behavior in the wild much less predictable than that under laboratory conditions [73]. In opposition to the vast human literature on the 'person-situation debate' [19,31,33,71,74], the

importance of environmental context in shaping individual animal behavior remains descriptive [24] and experimentally largely unexplored, with few exceptions [21,22,27,75]. Here we closed this gap in knowledge by quantitatively demonstrating how situational environmental and locomotor context changes individual behavior and individuality in animals. Our results demonstrate that situational environmental context has a pronounced effect on individual behavioral responses, be it an alternative stimulus representation, a different arena, or another locomotive modality.

Similar to the human literature [19], the correlation coefficients are lower across situations than in the same situation or environmental context. From this, we can conclude that under more natural conditions with varying contexts, the stability of individual traits will be reduced but remain measurable; therefore, for each situational context, the brain computes the appropriate behavior. This is like the situation-behavior profile of the individual in the personality psychology literature [76,77]. Each time the individual is placed in the same situational context, the same behavior will be evoked, in a different context, a modified behavior. But despite these modifications, the individual remains stable. In line with this, a vast literature demonstrates the importance of animal individual differences for ecological communities under natural conditions reviewed in: [20,78].

Our quantitative analysis of the effect of environmental and locomotor context on behavioral stability revealed a hierarchy. As expected from animal and human studies, the time frame of days had little effect on the behavioral outcome [8,10,13,19,32,72,79]. The hierarchy revealed by our experiments argues for differences in the relevance of environmental features for the traits we measured, which aligns with Mischel's strong or weak situations [80]. Therefore, it is unsurprising that exploration can be best measured across situations within experiments of walking flies, and attention towards a stimulus can be measured across movement modalities. Our quantitative analysis demonstrates that situational context can be the most significant factor in determining the individual behavioral outcome, even in a per-design visual assay. This argues that individual behavior is determined by the entirety of the situation consisting of both the stimulus and the environmental context. For each situation, each individual manifests its individual behavior.

In the future, it will be important to investigate which individual neurophysiological responses change when tested under exactly the same stimulus, but different situations. A systematic analysis of relevant circuit elements for different behaviors will allow for determining the exact neuronal substrates underlying individual behavioral computations within a fly's or other animals' brains. This future research on animal models will provide important new insight into the 'person-situation debate'.

On a more practical level, the importance of the situational environmental context for shaping individual behavioral outcomes is also very important when comparing the results of different research groups when using similar behavioral paradigms. In many instances, it is impossible to replicate all components of a specific assay, let alone the conditions of the experimental room. Our results show that such details substantially impact individual behavioral responses and contribute to errors in replicating the results from another lab [81,82]. Only meticulous and detailed reporting of as many environmental features as possible will hopefully alleviate some of these problems in the future.

In conclusion, our work confirms that animals including flies have, like humans, individuality across situations. Similar to humans, animal individuality across situations is also marked by lower correlation coefficients than repetitions of a single situation. The individual is stable across situations producing individualistic behavior through an interaction with the situation. This involves a hierarchy of influence of different environmental features on the predictability of behavior across situations.

Acknowledgements

The authors thank the Bloomington stock center and Eugenia Chiappe for fly stocks and reagents. This work was supported by the Deutsche Forschungsgemeinschaft (DFG) through the DFG research unit 5289 RobustCircuit (G.A.L, M.F.W), through grants LI 2640/1-1, FOR5289 LI 2640/2-1 (G.A.L.), WE 5761/2-1 and WE 5761/4-1 (M.F.W.), SPP 2205 (M.F.W.), through AFOSR grant FA9550-19-1-7005 (M.F.W.), and with support from the Fachbereich Biologie, Chemie & Pharmazie of the Freie Universität Berlin, as well as the Division of Neurobiology at Freie Universität Berlin. We thank members of the Linneweber and Wernet labs, Randolf Menzel and Robin Hiesinger for helpful discussions.

Author Contributions

Conceptualization, T.F.M., G.A.L. and M.F.W.; Methodology, T.F.M., G.A.L. and M.F.W.; Investigation, T.F.M., C.K., M.A.H., F.F., T.M.; Resources, M.F.W.; T.F.M., G.A.L. and M.F.W.; Supervision, G.A.L. and M.F.W.; Funding Acquisition, M.F.W. and G.A.L

Declaration of Interests

The authors declare no competing interests.

Figure 1:

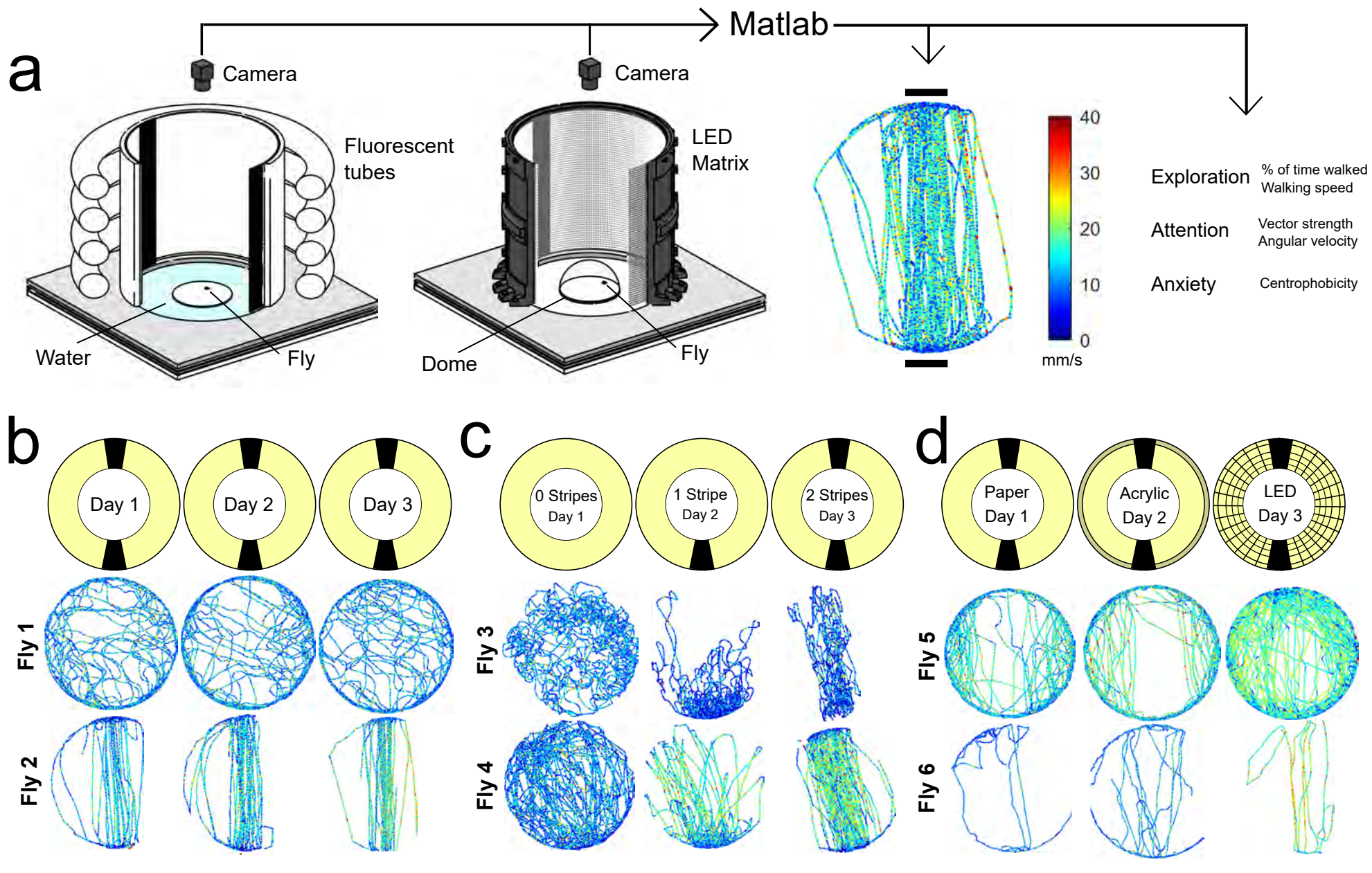
a
Matlab
Camera
Camera
Fluorescent tubes
LED Matrix
Water
Fly
Dome
Fly
40
30
20
10
0
mm/s
Exploration
% of time walked
Walking speed
Attention
Vector strength
Angular velocity
Anxiety
Centrophobicity
b
Day 1
Day 2
Day 3
Fly 1
Fly 2
c
0 Stripes Day 1
1 Stripe Day 2
2 Stripes Day 3
Fly 3
Fly 4
d
Paper Day 1
Acrylic Day 2
LED Day 3
Fly 5
Fly 6

Figure legends

Fig. 1: Setups for studying individuality walking flies. **a** Overview of a classical (left, fluorescent tubes) and LED (middle) Buridan assay (behavioral platform diameter = 120mm). A MATLAB script provides single fly tracking and analysis of behavioral key components (right). **b-d** persistence of individual walking patterns across time (**b**), different stripe numbers (**c**), and changes in background illumination (**d**).

Figure 2:

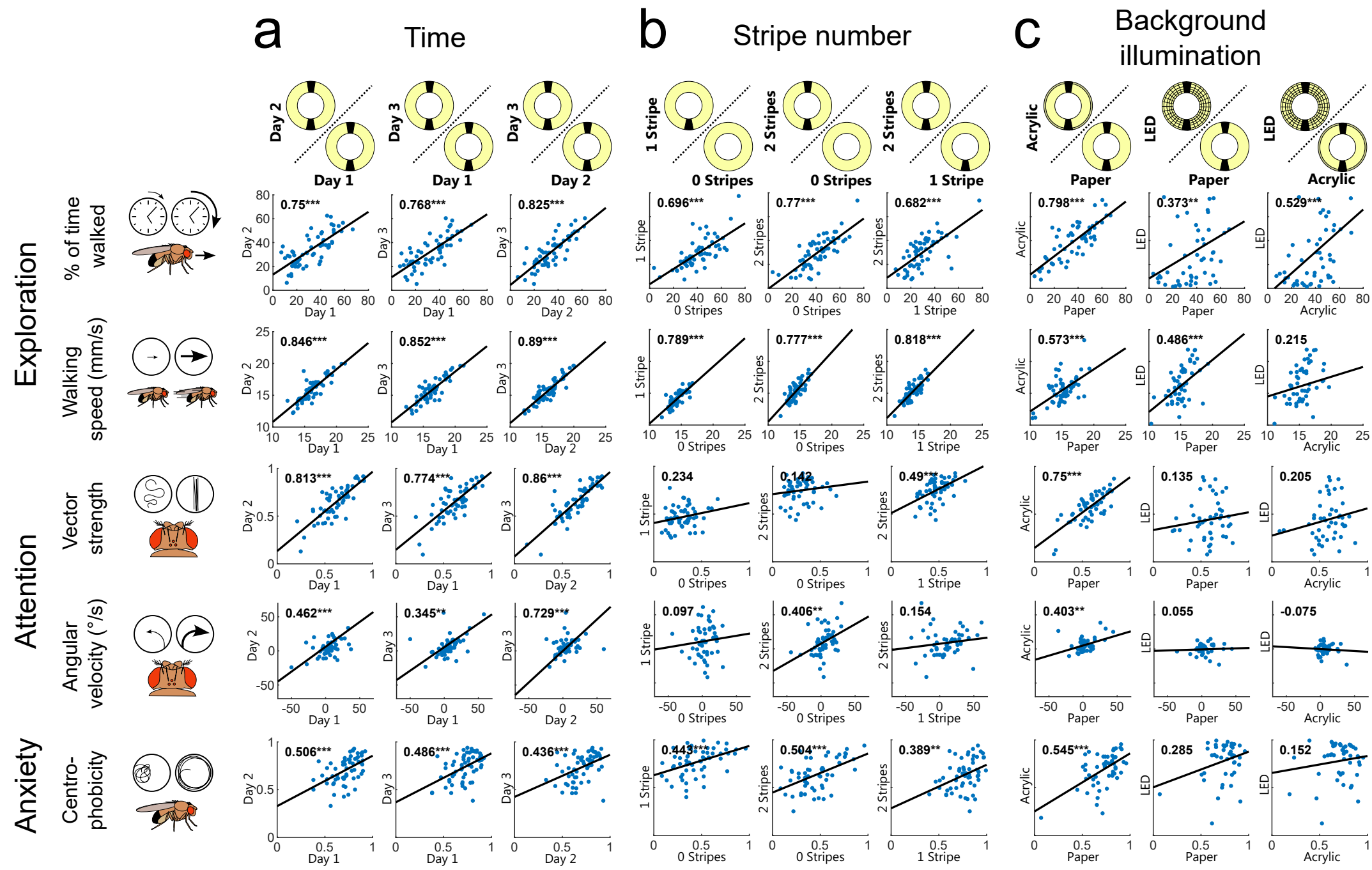
a
Time
b
Stripe number
c
Background illumination
Day 2
Day 3
Day 3
1 Stripe
2 Stripes
2 Stripes
Acrylic
LED
LED
Day 1
Day 1
Day 2
0 Stripes
0 Stripes
1 Stripe
Paper
Paper
Acrylic
Exploration
% of time walked
0.75***
0.768***
0.825***
0.696***
0.77***
0.682***
0.798***
0.373**
0.529***
Walking speed (mm/s)
0.846***
0.852***
0.89***
0.789***
0.777***
0.818***
0.573***
0.486***
0.215
Attention
Vector strength
0.813***
0.774***
0.86***
0.234
0.142
0.49***
0.75***
0.135
0.205
Angular velocity (°/s)
0.462***
0.345**
0.729***
0.097
0.406**
0.154
0.403**
0.055
-0.075
Anxiety
Centro-phobicity
0.506***
0.486***
0.436***
0.443***
0.504***
0.389**
0.545***
0.285
0.152

Fig. 2: Individual traits of walking flies persist over time but depend on the visual scenery. **a-c** Correlation of key behavioral parameters over time (**a**), different stripe numbers (**b**), and changes in background illumination (**c**). Correlation coefficients are displayed in the upper left corner of each plot. *=p<0.05, **=p<0.01, ***=p<0.001, for detailed fly numbers per experimental condition, see supplemental Fig. S2.

Figure 3:

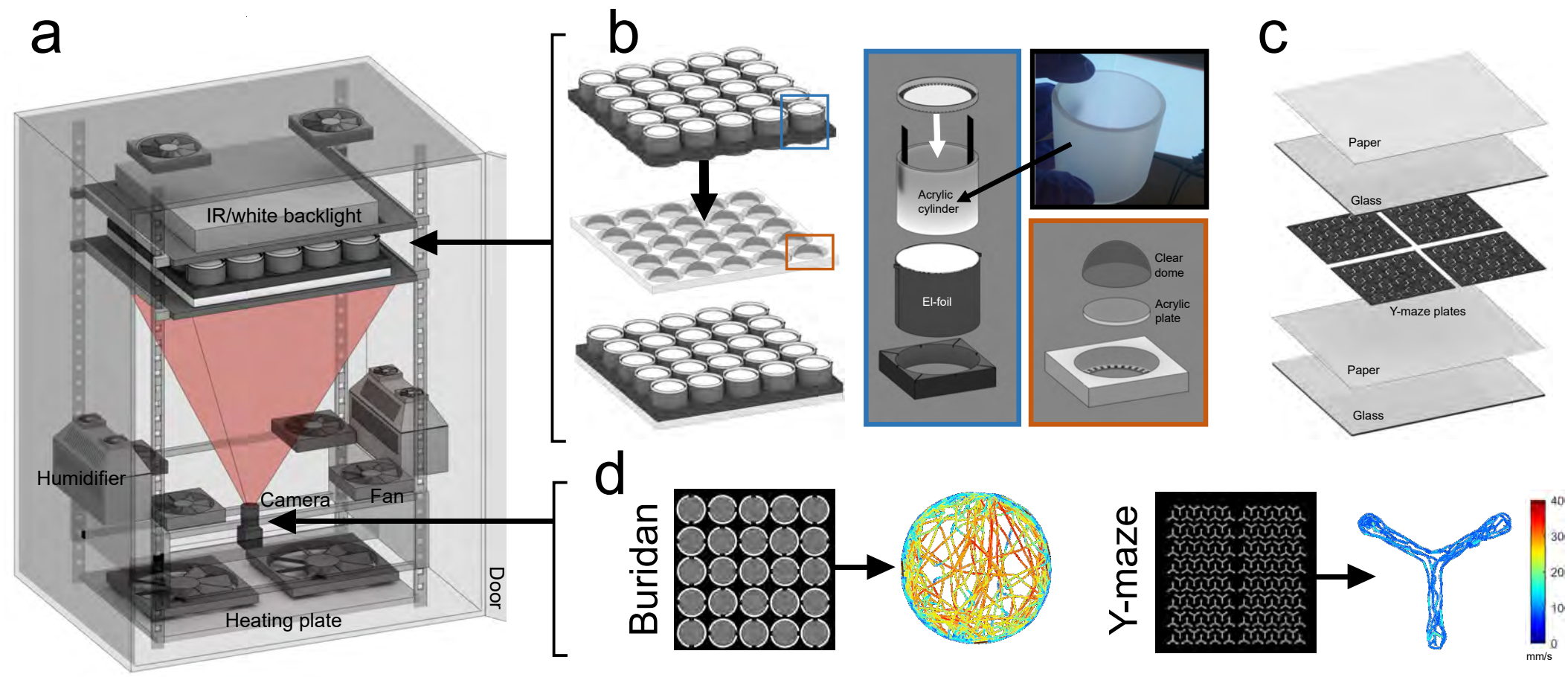
a
IR/white backlight
Humidifier
Camera
Fan
Heating plate
Door
b
Acrylic cylinder
El-foil
Clear dome
Acrylic plate
c
Paper
Glass
Y-maze plates
Paper
Glass
d
Buridan
Y-maze
40
30
20
10
0
mm/s

Fig. 3: A high-throughput assay for studying the influence of temperature, illumination, and arena shape on individuality. **a** Setup overview. Flies are filmed from below against a near-infrared backlight and are walking within a 5x5 array of small Buridan chambers (**b**) or one of up to 144 Y-maze arenas (**c**). The setup is housed within a temperature- and humidity-controlled enclosure (600 x 450 x 820 mm). The provided MATLAB code corrects lens distortions, automatically detects the arenas, and tracks each fly's position over time, allowing for generating high-throughput single-fly behavioral data (**d**).

Figure 4:

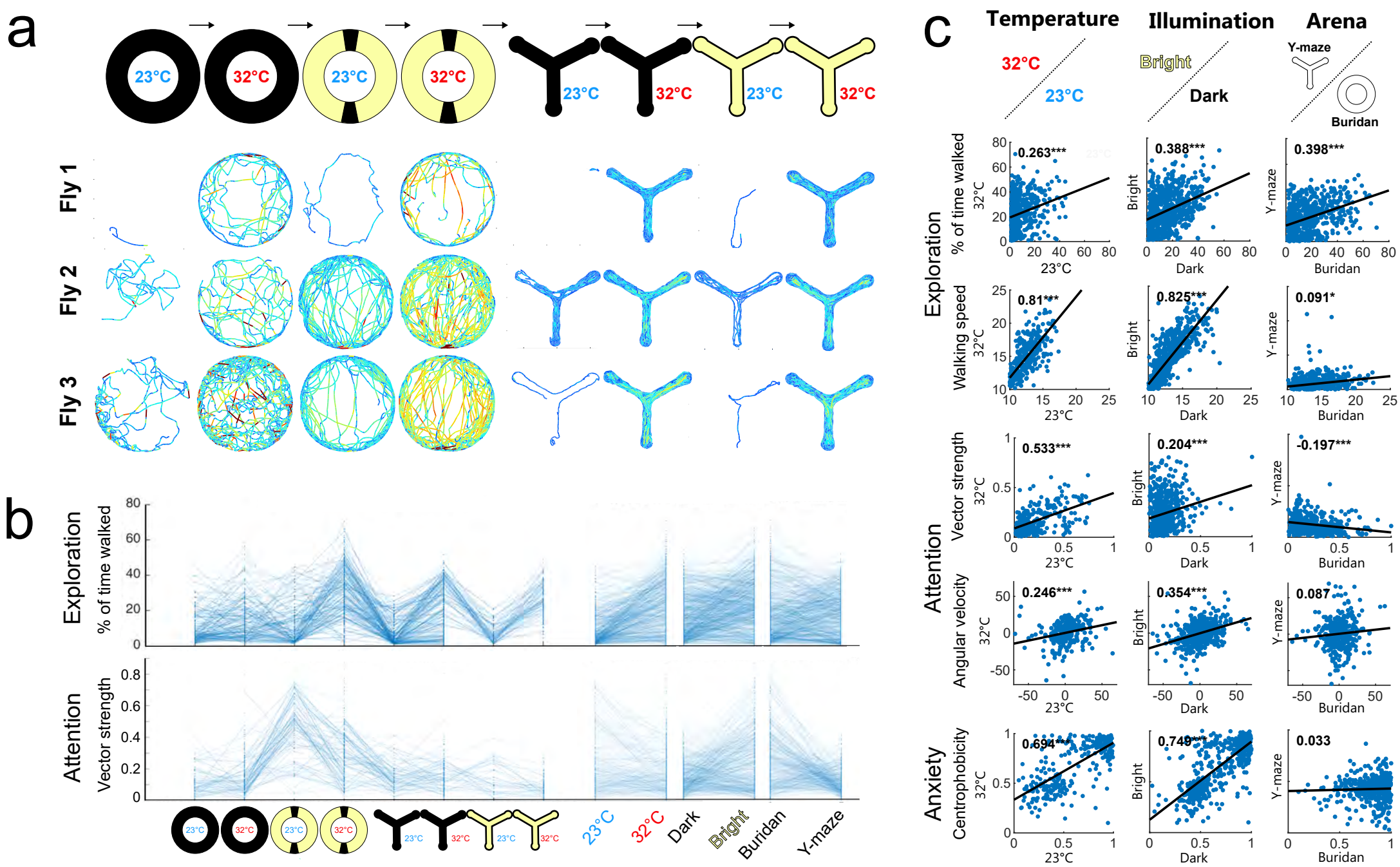
a
23°C
32°C
Fly 1
Fly 2
Fly 3
b
Exploration
% of time walked
Attention
Vector strength
Dark
Bright
Buridan
Y-maze
c
Temperature
Illumination
Arena
Y-maze
Buridan
Exploration
% of time walked
Walking speed
Attention
Vector strength
Angular velocity
Anxiety
Centrophobicity
0.263***
0.388***
0.398***
0.81***
0.825***
0.091*
0.533***
0.204***
-0.197***
0.246***
0.354***
0.087
0.694***
0.748***
0.033

Fig. 4: The influence of temperature, illumination, and arena shape on individuality in walking flies. **a** Individuality in walking patterns across different temperatures, illumination, and arena type. Diameter circular arena = 49mm, arm length from center Y-maze = 13.5mm. **b** changes in the % of time walked for all tested flies depending on environmental conditions. **c** Changes in the % of time walked grouped by temperature, illumination, and arena. **d** Correlation of key behavioral parameters across temperature, illumination, and arena type. For detailed fly numbers per experimental condition, see supplemental Fig. S6.

Figure 5:

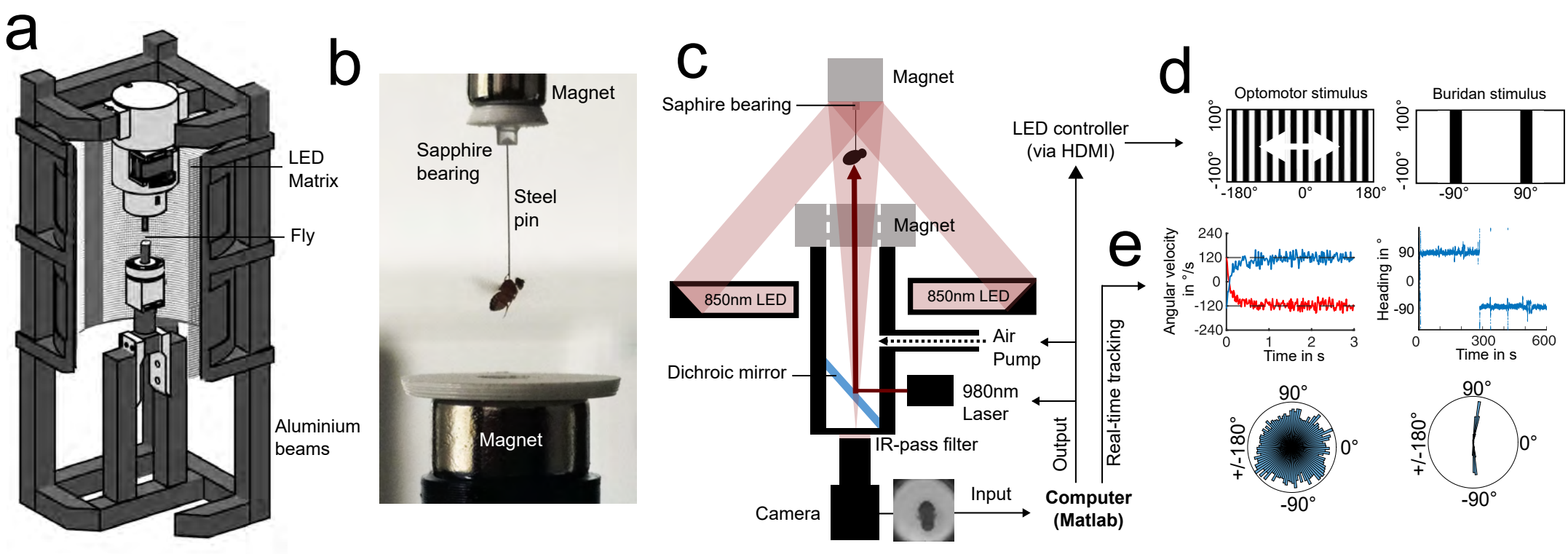
a
LED
Matrix
Fly
Aluminium
beams
b
Magnet
Sapphire
bearing
Steel
pin
Magnet
c
Magnet
Saphire bearing
Magnet
850nm LED
850nm LED
Air
Pump
Dichroic mirror
980nm
Laser
IR-pass filter
Camera
Input
Output
Real-time tracking
LED controller
(via HDMI)
Computer
(Matlab)
d
Optomotor stimulus
Buridan stimulus
100°
-100°
-180°
0°
180°
-90°
90°
e
Angular velocity
in °/s
240
120
0
-120
-240
0
1
2
3
Time in s
Heading in °
90
0
-90
0
300
600
Time in s
90°
+/-180°
0°
-90°
90°
+/-180°
0°
-90°

Fig. 5: A virtual flight simulator for studying individuality in flying flies. **a** Setup overview (225 x 225 x 600 mm). Flies are glued to a steel pin and placed in a magneto-tether surrounded by an LED matrix for stimulus presentation. **b** Close-up photo of a tethered flying fly. **c** Schematic setup overview. Flies are filmed from below through an IR-pass filter against near-infrared back illumination. A connected pump provides air puffs to reinitiate flight if necessary. We provide a mounting port for an optional IR-laser for heat punishment via a dichroic mirror. **d** A MATLAB script controls stimulus presentation (optomotor or Buridan stimulus) with an angular extent of 360° azimuthally and 100° vertically and provides simultaneous real-time tracking of flight-heading over 360° (**e**). Before an experiment, each fly's ability to rotate was tested using a 120°/s CW or CCW stripe rotation (optomotor stimulus), resulting in measured rotational flight movements close to the rotational velocity of the stripe pattern (**e**, upper left) and uniform distribution of angles (**e**, lower left). This was followed by each fly flying under the Buridan stimulus for 10min (**d**, right) and an analysis of heading choices (**e**, upper right) and their angular distribution (**e**, lower right).

Figure 6:

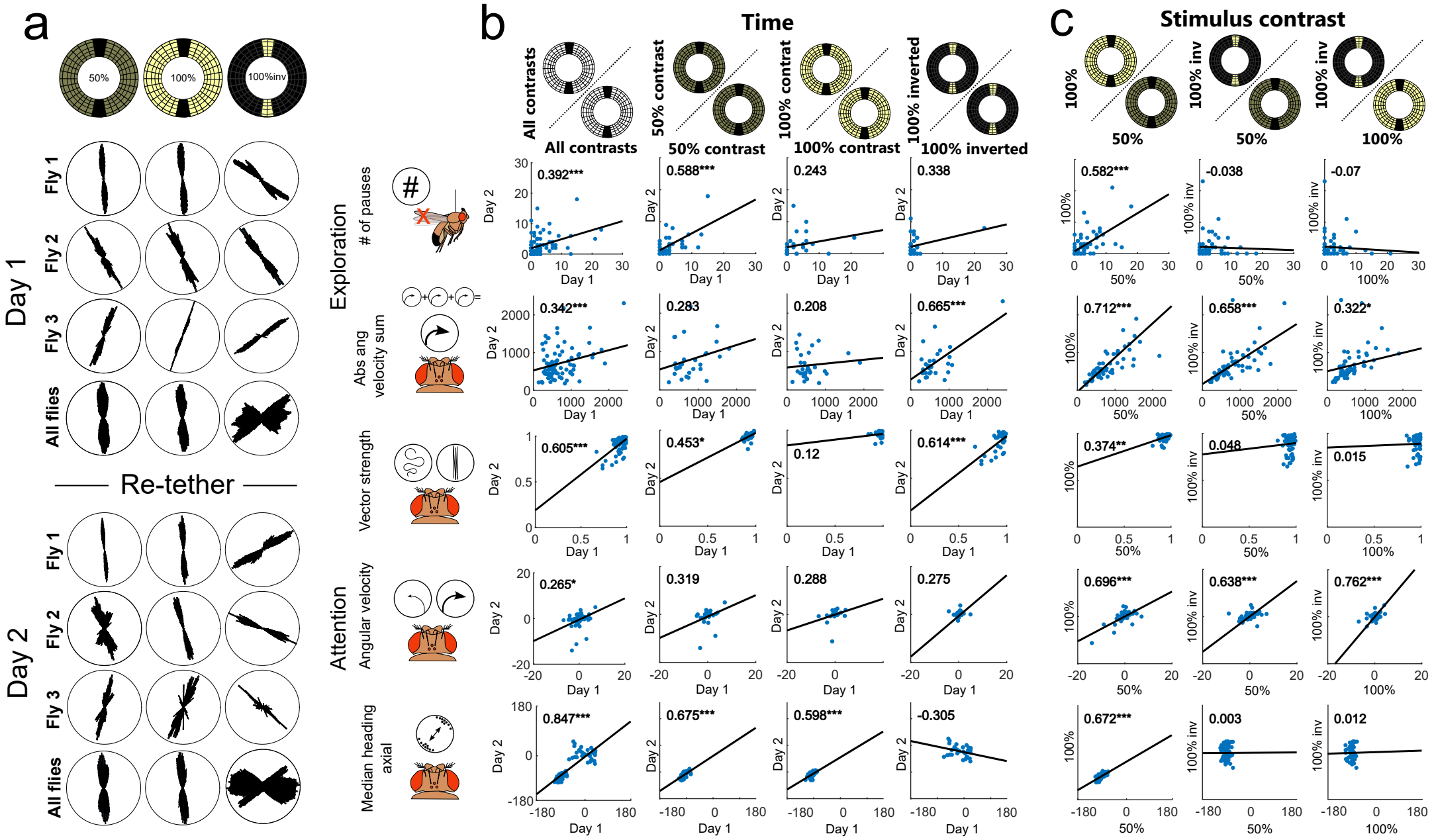
a
50%
100%
100%inv
Day 1
Fly 1
Fly 2
Fly 3
All flies
Re-tether
Day 2
Fly 1
Fly 2
Fly 3
All flies
b
Time
All contrasts
50% contrast
100% contrast
100% inverted
Exploration
# of pauses
Abs ang velocity sum
Vector strength
Attention
Angular velocity
Median heading axial
Day 1
Day 2
0.392***
0.588***
0.243
0.338
0.342***
0.283
0.208
0.665***
0.605***
0.453*
0.12
0.614***
0.265*
0.319
0.288
0.275
0.847***
0.675***
0.598***
-0.305
c
Stimulus contrast
100%
50%
100% inv
0.582***
-0.038
-0.07
0.712***
0.658***
0.322*
0.374**
0.048
0.015
0.696***
0.638***
0.762***
0.672***
0.003
0.012

Fig. 6: Individual traits of flying flies persist over time but depend on the visual scenery. **a** Angular histograms show the persistence of individual heading choices over consecutive days and across different contrast ratios. **b,c** Correlation of key behavioral parameters over time (**b**) and depending on changes in visual contrast (**c**). For detailed fly numbers per experimental condition, see supplemental Fig. S10.

Figure 7:

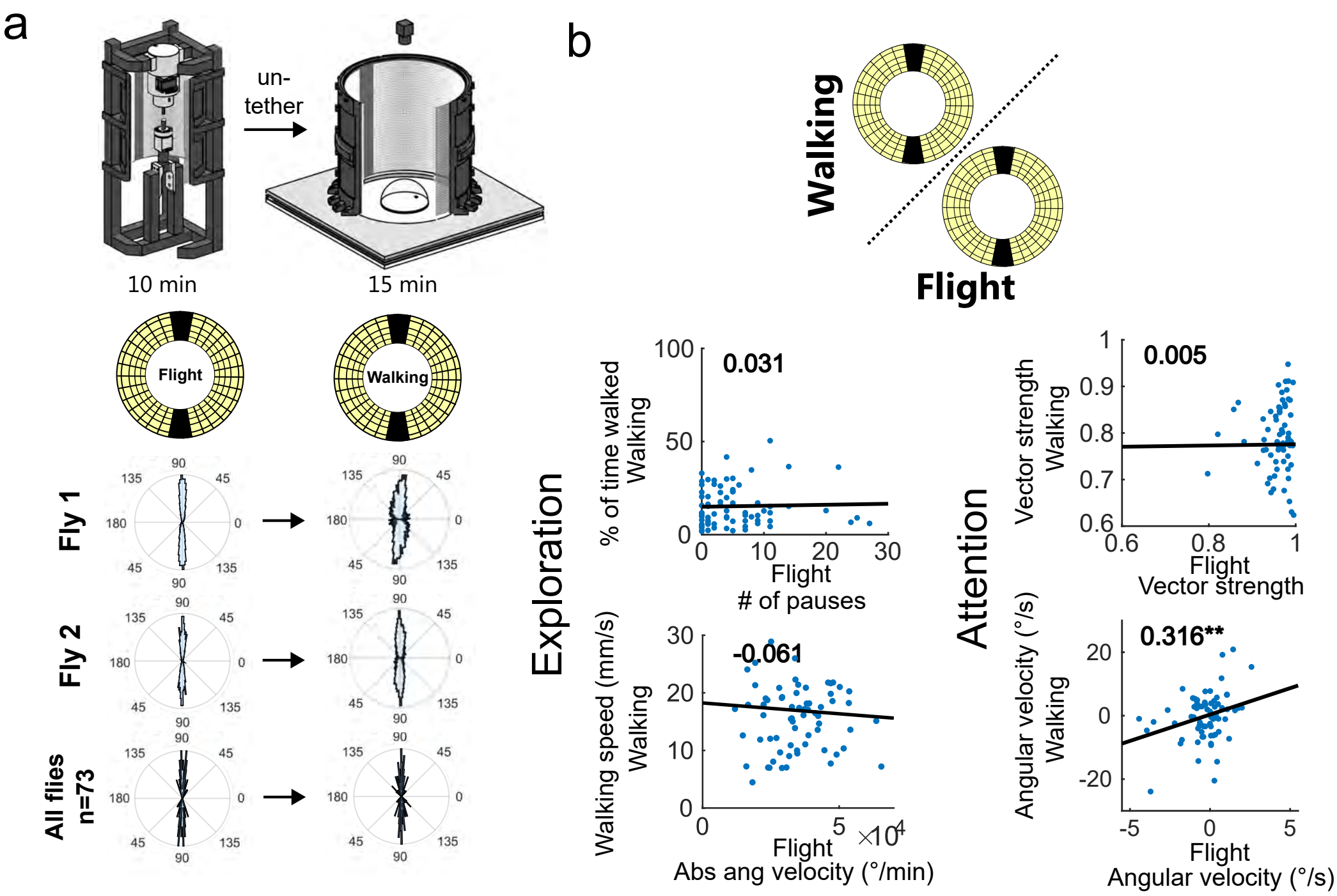
a
un-
tether
10 min
15 min
Flight
Walking
Fly 1
Fly 2
All flies
n=73
b
Walking
Flight
Exploration
Attention
0.031
% of time walked
Walking
Flight
# of pauses
0.005
Vector strength
Walking
Flight
Vector strength
-0.061
Walking speed (mm/s)
Walking
Flight
Abs ang velocity (°/min)
0.316**
Angular velocity (°/s)
Walking
Flight
Angular velocity (°/s)

Fig. 7: Visual attention persists across different behavioral states. **a** Experimental overview. Flies were untethered after flying within the flight simulator for 10 min (left) and walking for 15 min (right) under the same Buridan stimulus (stripe size=11°). Single fly data (middle) and population data (bottom) reveal stripe fixation behavior when walking and during flight. **b** Correlation of key behavioral parameters depending on the behavioral state (flight=x-axis, walking=y-axis). For detailed fly numbers per experimental condition, see supplemental Fig. S12.

Figure 8:

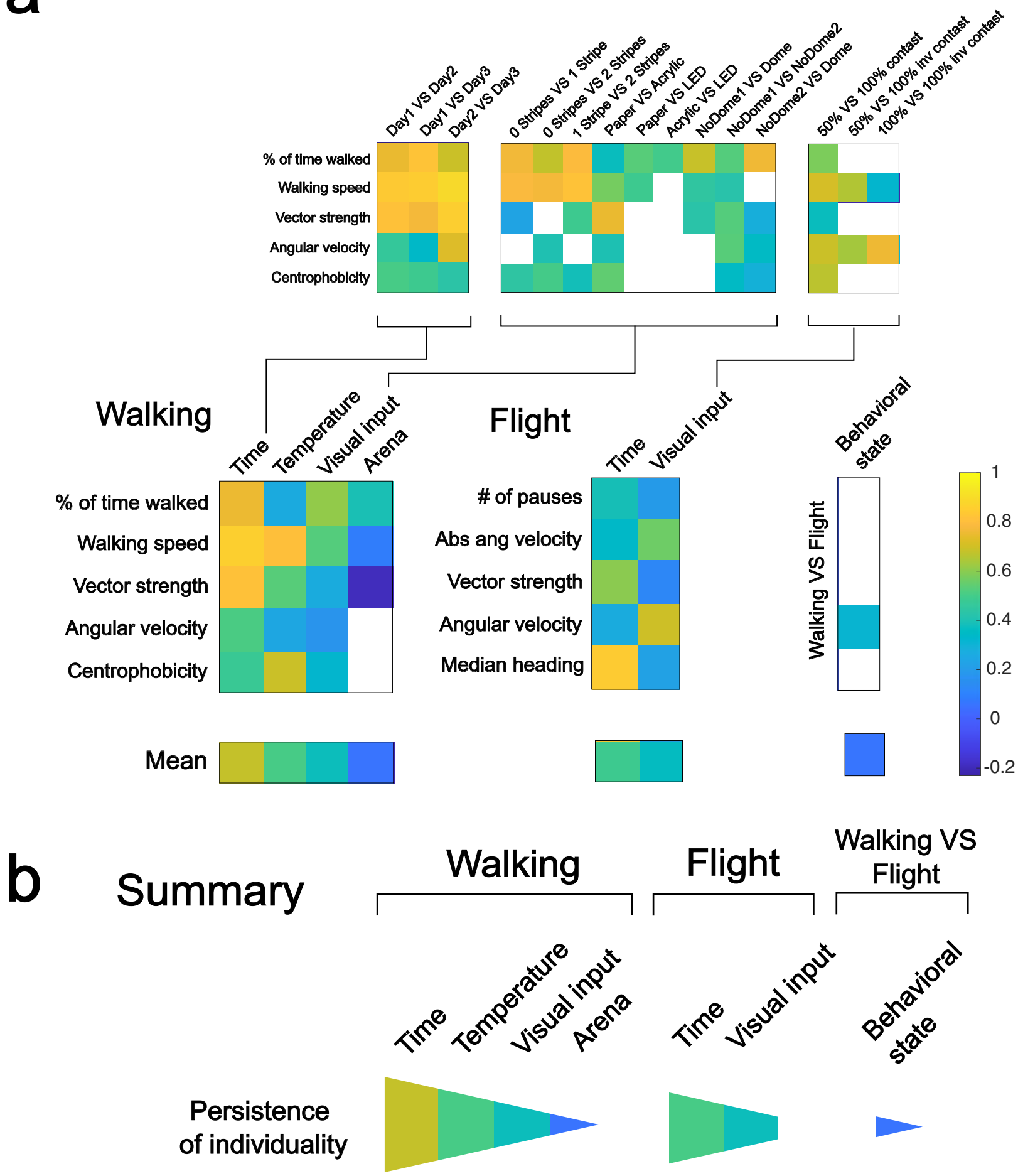
a
Day1 VS Day2
Day1 VS Day3
Day2 VS Day3
0 Stripes VS 1 Stripe
0 Stripes VS 2 Stripes
1 Stripe VS 2 Stripes
Paper VS Acrylic
Paper VS LED
Acrylic VS LED
NoDome1 VS Dome
NoDome1 VS NoDome2
NoDome2 VS Dome
50% VS 100% contast
50% VS 100% inv contast
100% VS 100% inv contast
% of time walked
Walking speed
Vector strength
Angular velocity
Centrophobicity
Walking
Time
Temperature
Visual input
Arena
Flight
Time
Visual input
Behavioral state
# of pauses
Abs ang velocity
Vector strength
Angular velocity
Median heading
Walking VS Flight
Mean
1
0.8
0.6
0.4
0.2
0
-0.2
b
Summary
Walking
Flight
Walking VS Flight
Time
Temperature
Visual input
Arena
Time
Visual input
Behavioral state
Persistence of individuality

Fig. 8: A hierarchy of environmental and behavioral contexts based on their influence on individuality. **a** Overview summarizing correlation coefficients ($p<0.05$) for key behavioral parameters depending on behavioral context, time, temperature, and visual input. **b** Quantification of the influence of behavioral and environmental contexts on the persistence of individuality.

Supplemental figure S1:

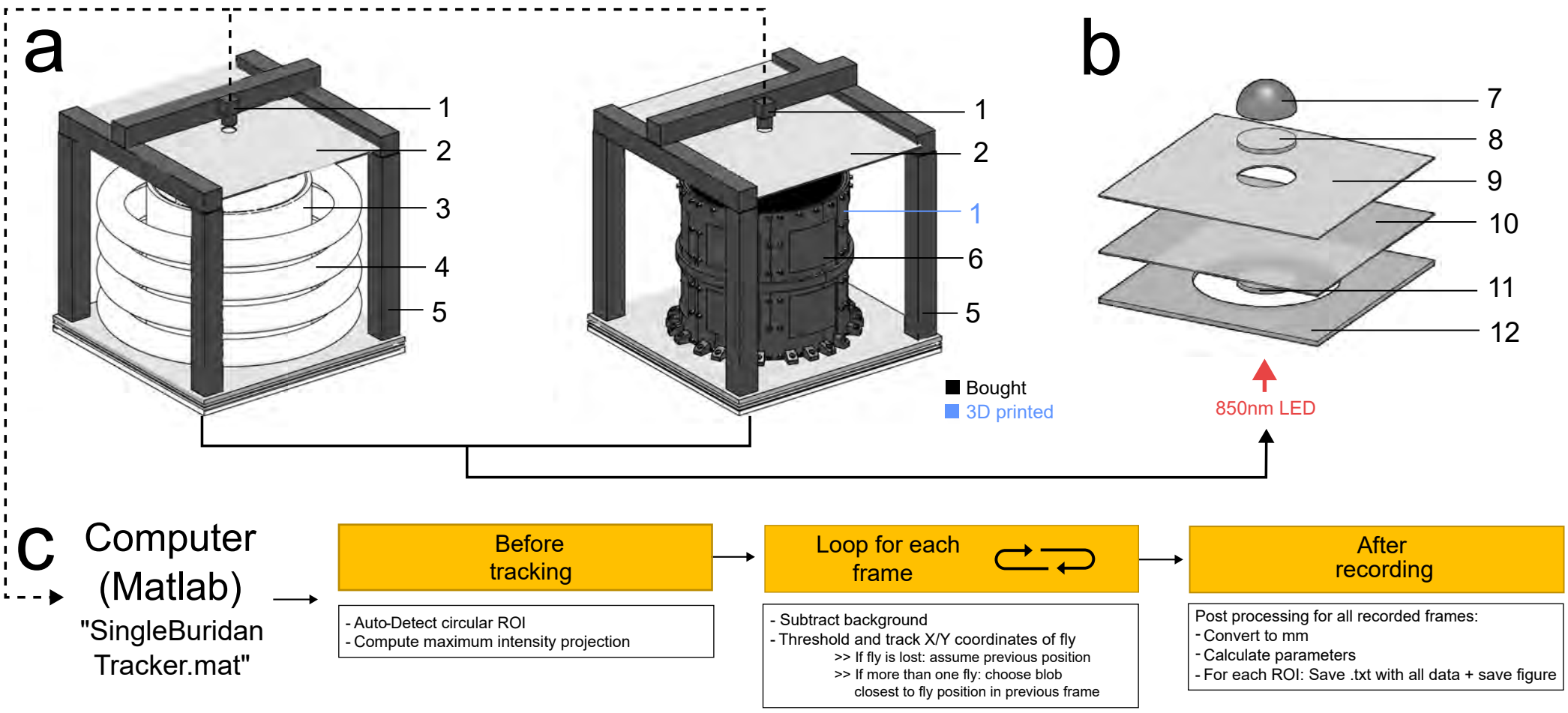

Supplemental figure legends

Supplemental Fig. S1: Construction of Buridan assays. **a** Two different types of Buridan assays (fluorescent tubes left, flexible LED matrix right) and the parts necessary for construction. Part numbers are referenced in supplemental table T2 and for 3D printed parts under github.com/LinneweberLab/individuality-assays for replication. Black numbers indicate off-the-shelve parts; blue numbers indicate 3D-printed parts. **b** construction of Buridan bottom plates. An 850nm LED strip is wrapped around a translucent acrylic disk (11), providing homogeneous near-infrared background illumination from below. **c** schematic illustration of the tracking procedure. The provided MATLAB script automatically reads video frames, tracks the X- and Y-coordinates of individual flies over time, and saves data for further analysis.

Supplemental figure S2:

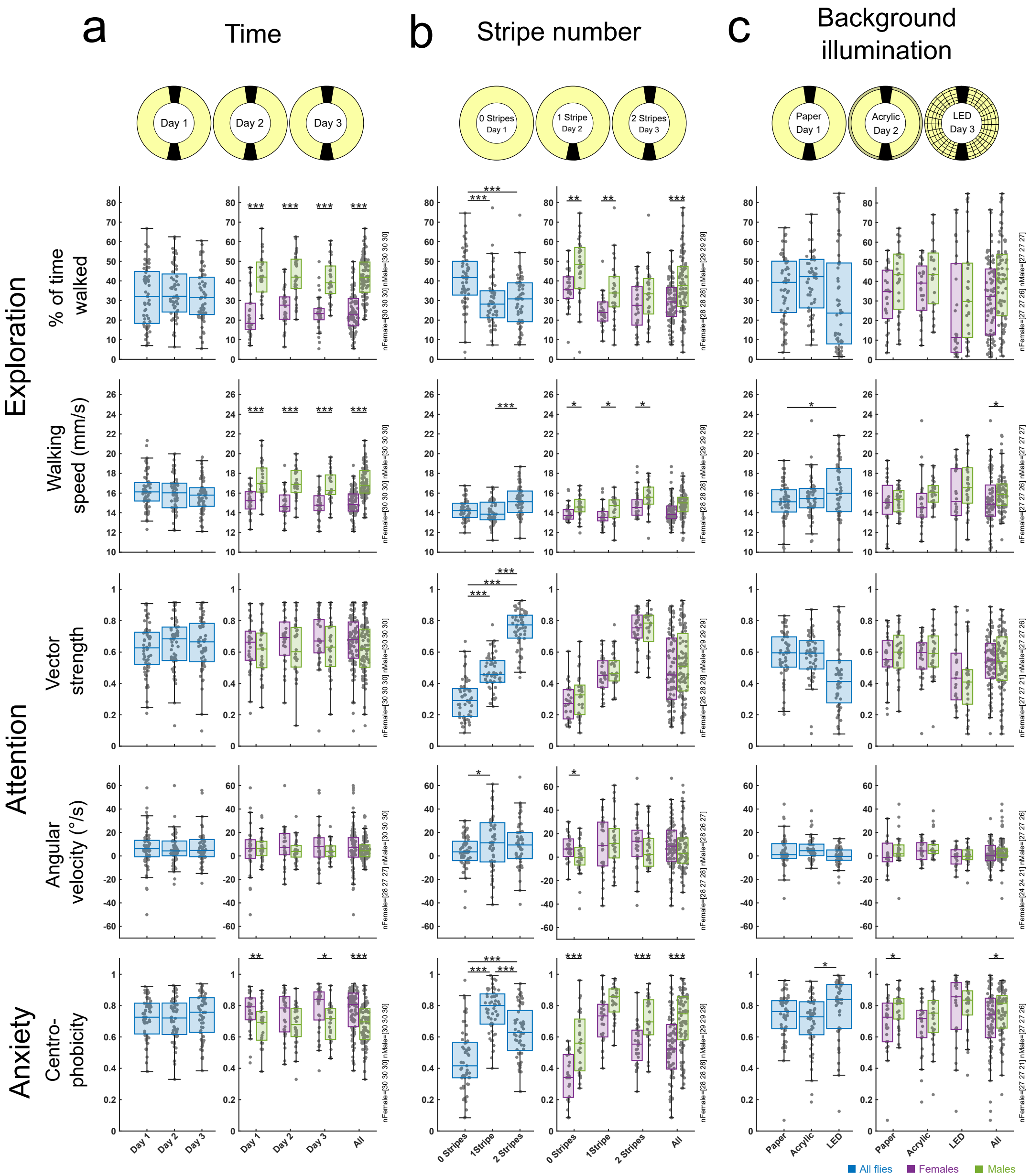

Supplemental Fig. S2: Population responses over time, varying stripe numbers and background illumination. **a-c** Boxplots illustrating key behavioral parameters for the whole population (blue) and separately for females/males (green/magenta) over time (**a**), varying stripe numbers (**b**) and background illumination (**c**). Animal numbers are indicated next to each plot.

Supplemental figure S3:

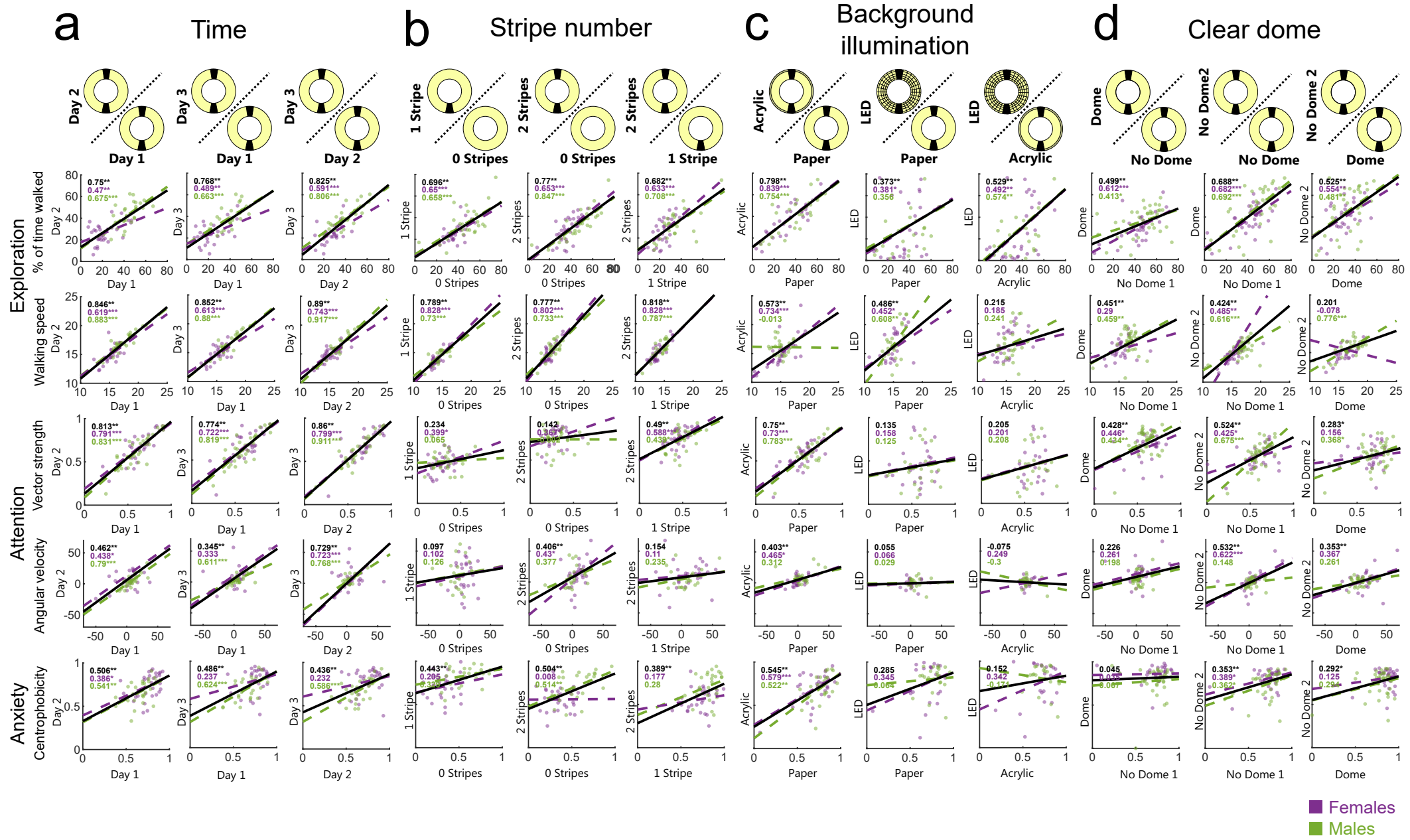

Supplemental Fig. S3: Sex-specific differences in individual traits. **a-d** Correlation of key behavioral parameters for females and males over time (**a**), different stripe numbers (**b**), changes in background illumination (**c**), and depending on the usage of a clear dome around the arena (**d**). Magenta=females, green=males. Correlation coefficients are displayed in the upper left corner of each plot. *=p<0.05, **=p<0.01, ***=p<0.001, for detailed fly numbers per experimental condition, see supplemental Fig. S2.

Supplemental figure S4:

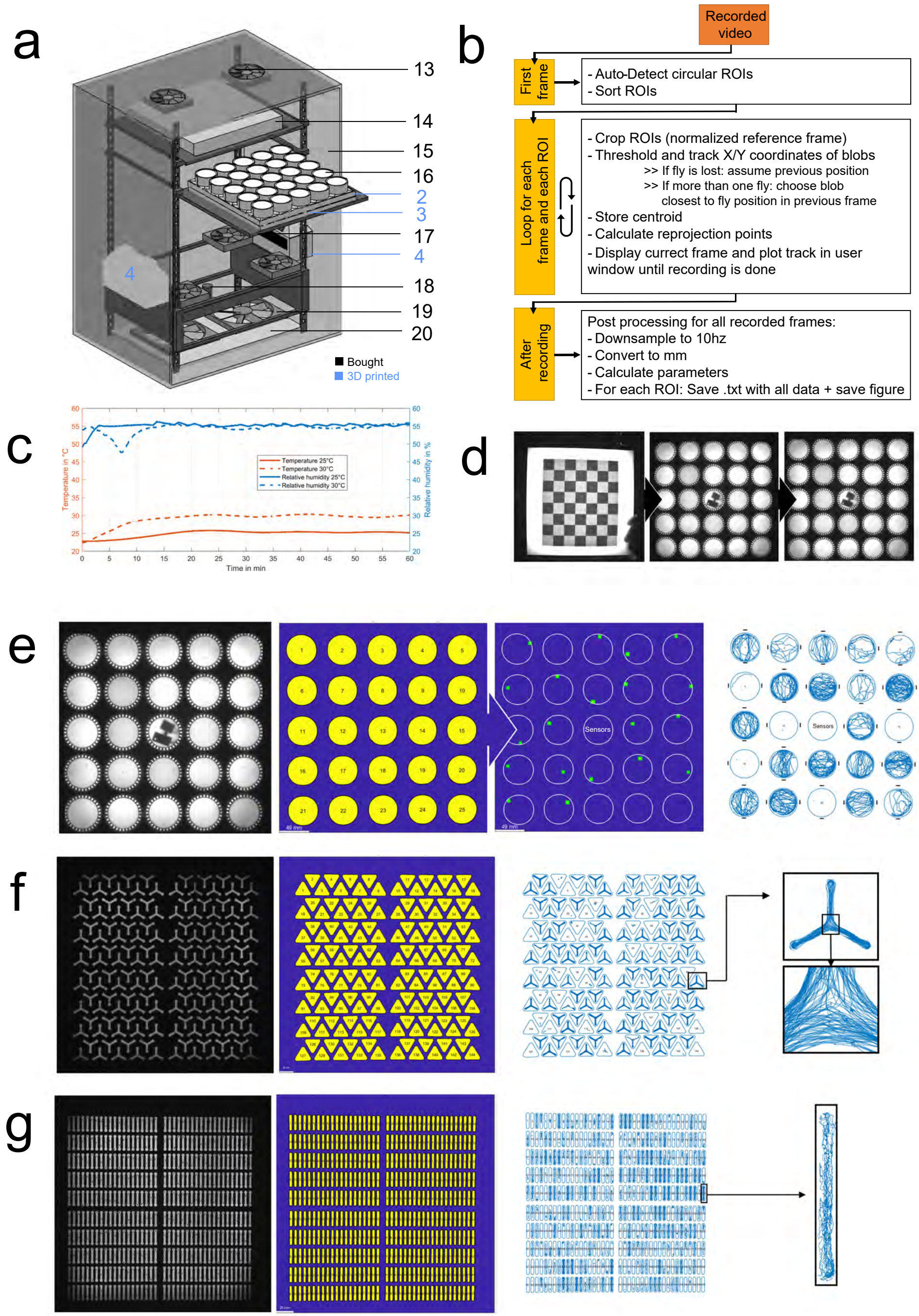

Supplemental Fig. S4: Construction of a high-throughput assay for studying the influence of temperature, illumination, and arena shape on individuality. **a** Overview of parts necessary for constructing the assay. Part numbers are referenced in supplemental table T2 and for 3D printed parts under github.com/LinneweberLab/individuality-assays for replication. Black numbers indicate off-the-shelve parts; blue numbers indicate 3D-printed parts. **b** Schematic illustration of the tracking procedure. The provided MATLAB script automatically reads video frames, detects single arenas, tracks the X- and Y-coordinates of individual flies over time, and saves data for further analysis. **c** Exemplary temperature- and humidity curves were measured within the center arena during heat-up to 25 and 30°C, respectively. Stable plateaus are reached after ~20min. **d** The camera was calibrated using the MATLAB calibration toolbox. The provided MATLAB script uses these camera parameters to correct lens distortion artifacts during tracking. **e** Screenshots of the tracking procedure using the multi-Buridan assay. Arenas are detected automatically, and individual flies get thresholded after background subtraction, resulting in reliable trajectories of each individual fly. **f** Same as **e**, but for the Y-maze assay. The box on the right shows an enlarged depiction of a single arena. **g** Same as **e**, but for linear assays, demonstrating the usability of the setup with other arena shapes. The box on the right shows an enlarged depiction of a single arena.

Supplemental figure S5:

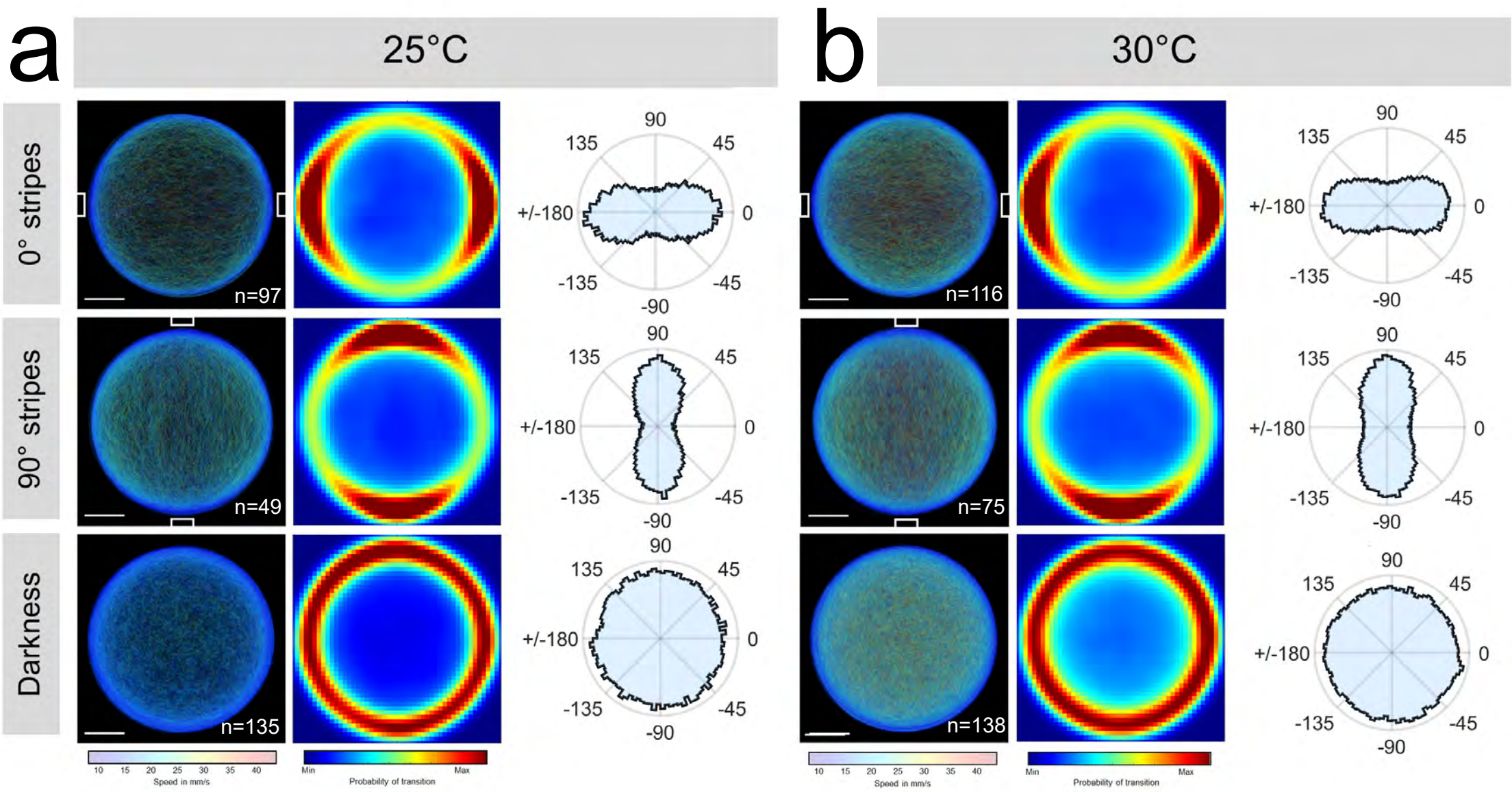

Supplemental Fig. S5: Preliminary data of a fly population (TopBanana) illustrating orientational responses. Flies walk between the 2 stripes and show randomly distributed headings in darkness, independent of temperature. **a** Velocity- (left, transparency added to tracks), transition- (middle), and angular plots (right, angles from moving periods only, non-axial) for vertical stripes positioned at 0° (top), 90° (middle) or in complete darkness (bottom), respectively for all tested flies at 25°C. Scale bar = 10mm. **b**) Same as **a**) but at 30°C. Fly numbers are indicated in the velocity plots.

Supplemental figure S6:

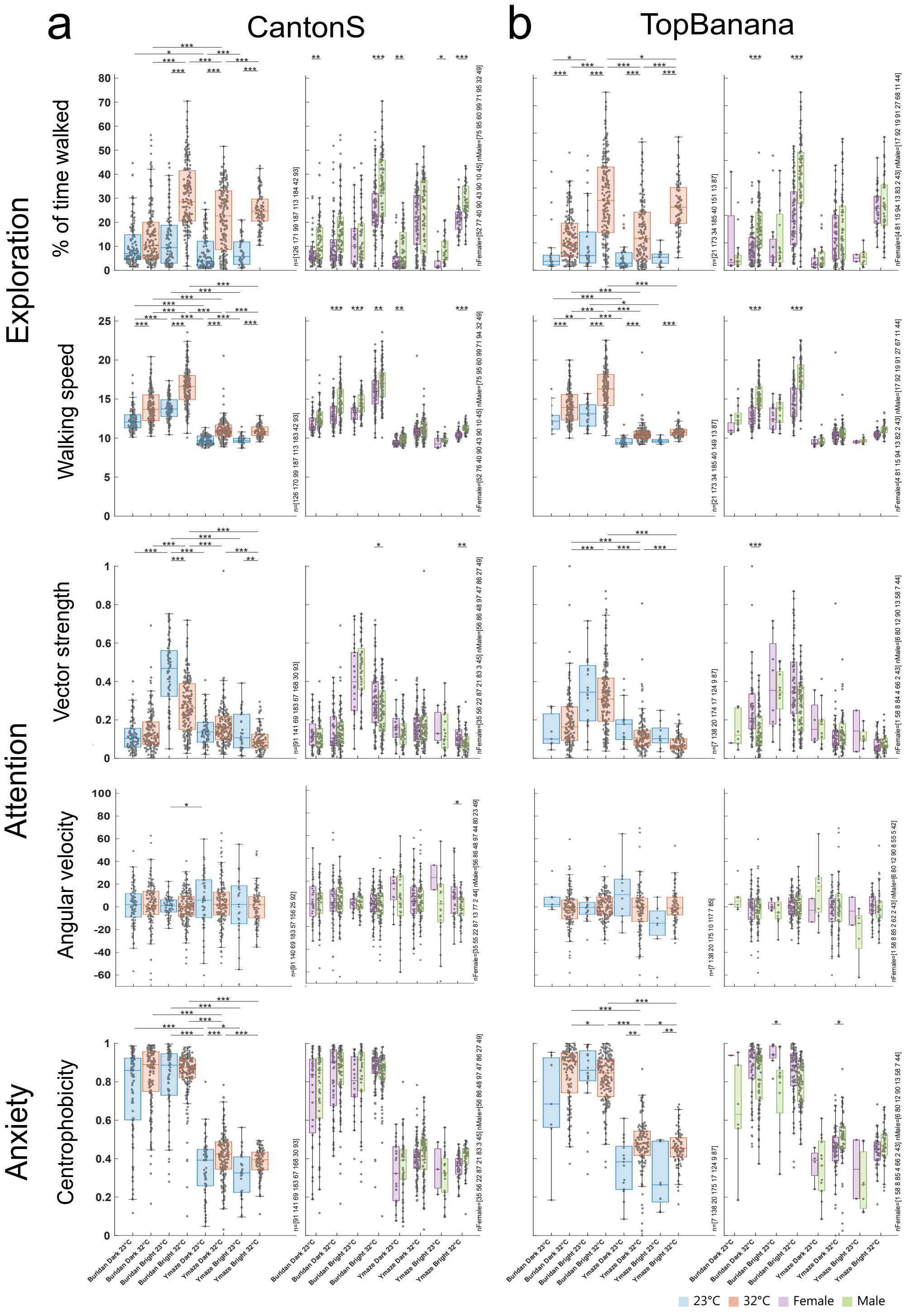

730 **Supplemental Fig. S6:** Sex- and genotype-specific population responses over varying temperature,
731 illumination and arena shape in walking flies. **a** Boxplots illustrating key behavioral parameters for the
732 whole tested CantonS population (left, blue=23°C, red=32°C) and separately for females/males
733 (green/magenta) over varying temperature, illumination and arena shape. Animal numbers are
734 indicated next to each plot. **b** Same as **a**, but for all tested TopBanana flies.

735

736

Supplemental figure S7:

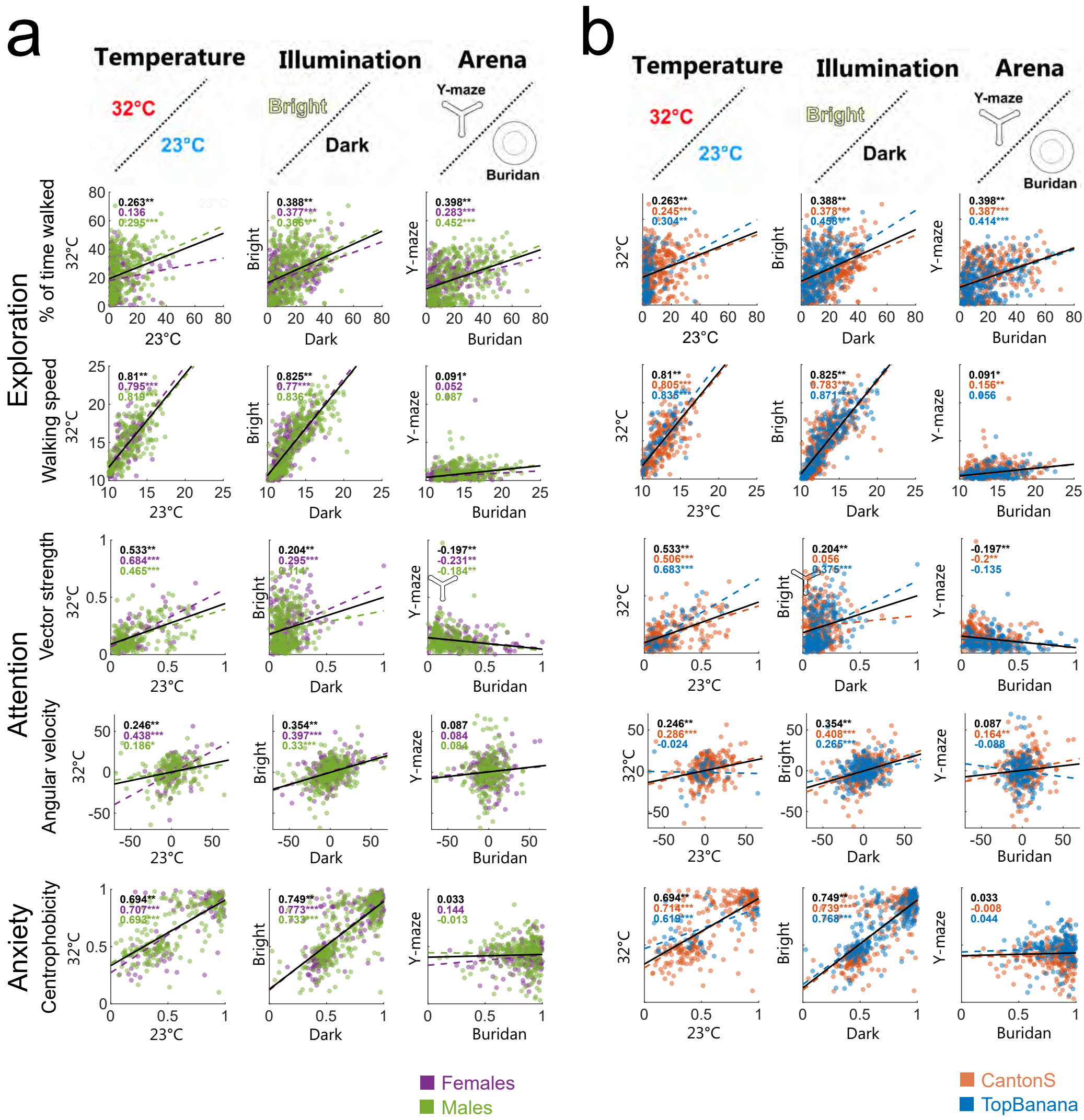

Supplemental Fig. S7: Sex- and genotype-specific differences based on the influence of temperature, illumination, and arena shape on the persistence of individual traits in walking flies. **a** Correlation of key behavioral parameters for females and males depending on temperature, illumination, and arena. Magenta=females, green=males. Correlation coefficients are displayed in the upper left corner of each plot. *=p<0.05, **=p<0.01, ***=p<0.001, for detailed fly numbers per experimental condition, see supplemental Fig. S6. **b** same as **a** but sorted by genotype (red=CantonS, blue=TopBanana).

Supplemental figure S8:

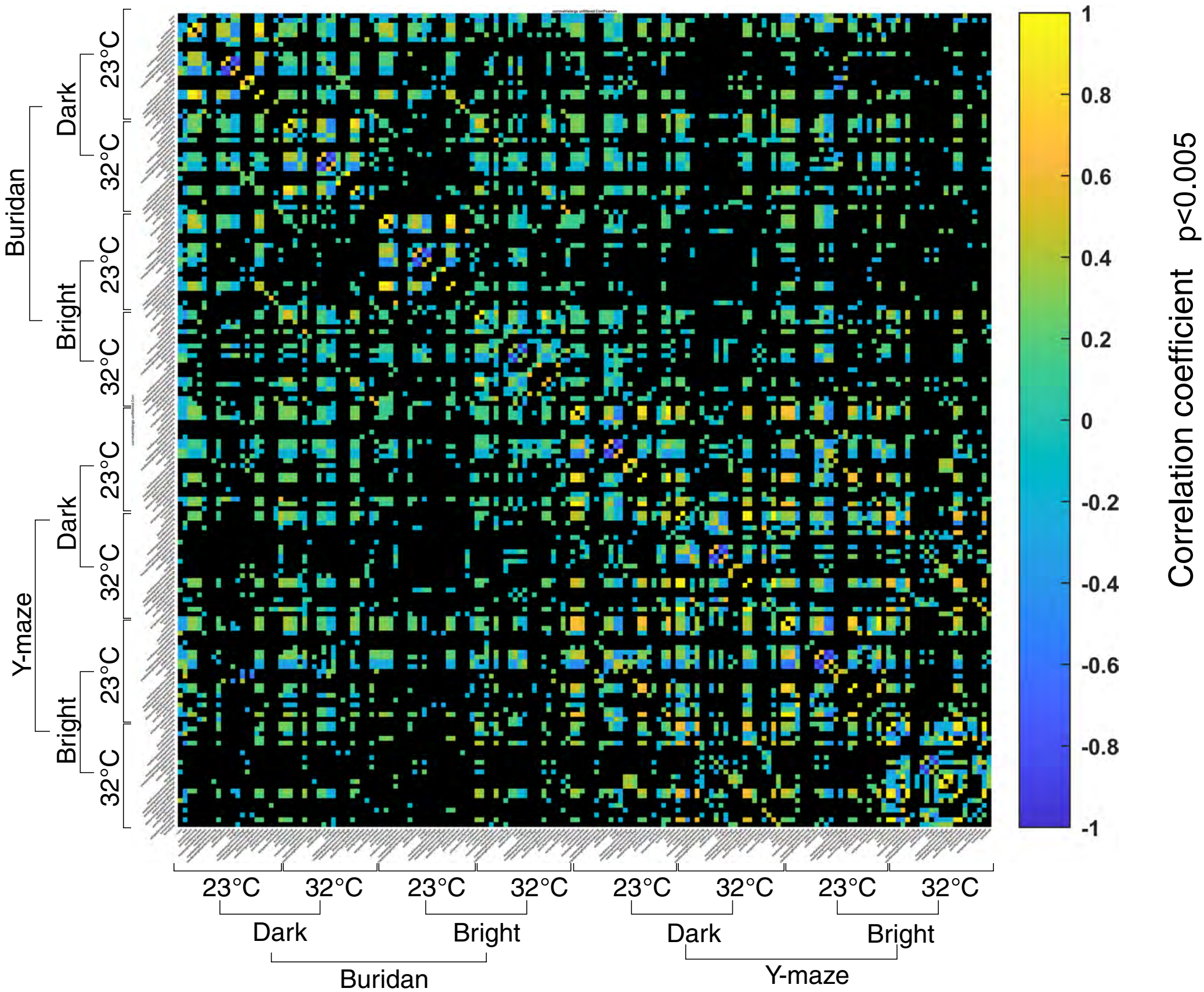

Supplemental Fig. S8: Complete correlation matrix across all behavioral parameters and contexts. Correlation coefficients with $p<0.05$ are color coded.

Supplemental figure S9:

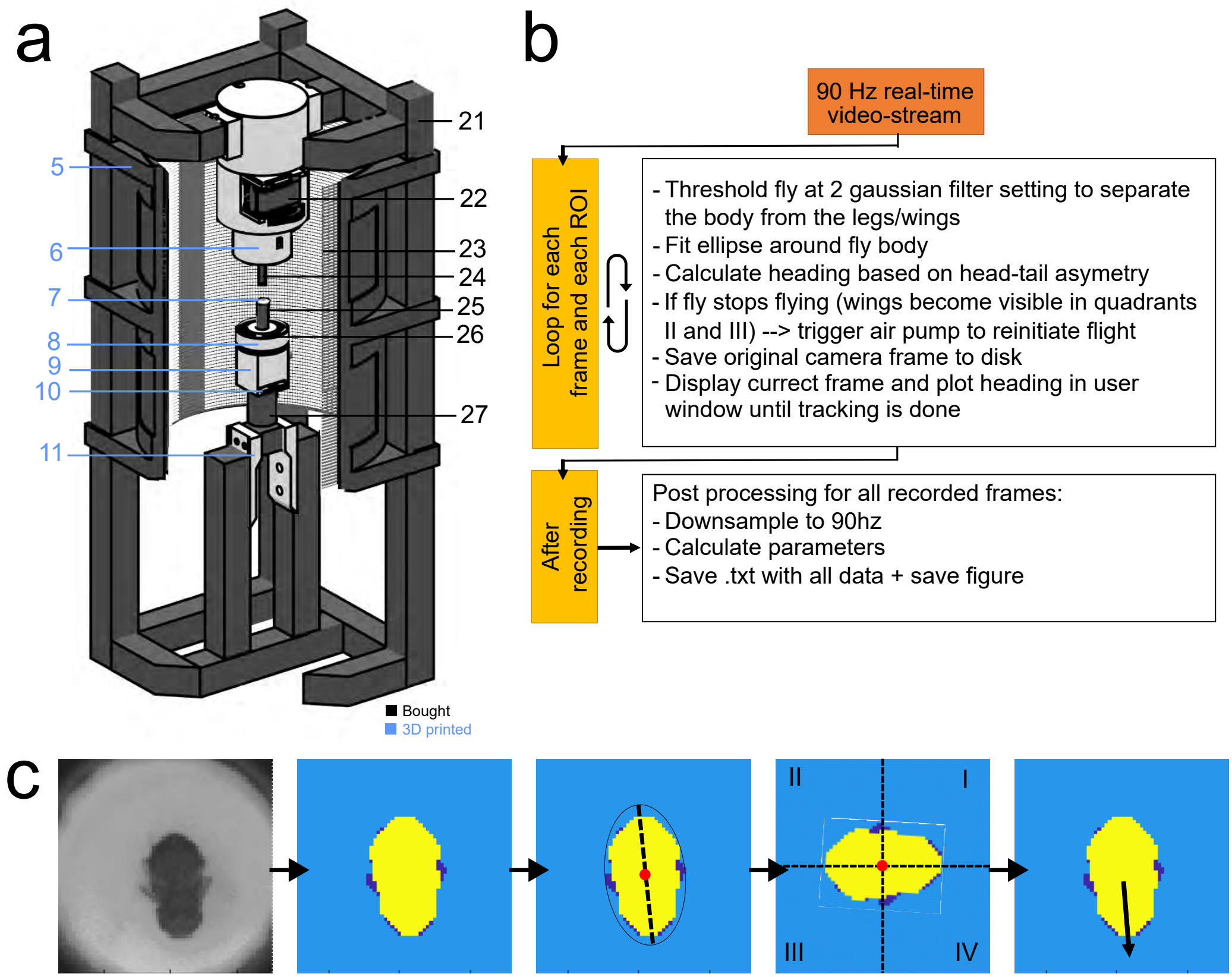

Supplemental Fig. S9: Construction of a virtual flight simulator for studying the persistence of individual traits in flying flies. **a** Overview of parts necessary for constructing the assay. Part numbers are referenced in supplemental table T2 and for 3D printed parts under github.com/LinneweberLab/individuality-assays for replication. Black numbers indicate off-the-shelve parts; blue numbers indicate 3D-printed parts. **b** schematic illustration of the tracking procedure. The provided MATLAB script works in real-time at ~90Hz on a 4GHz processor. The code automatically reads camera frames, computes the heading angle over time, and saves data for further analysis. **c** Illustration of the tracking procedure. The camera frame is thresholded using 2 different Gaussian filter settings to separately threshold the body (yellow) and legs/wings (dark blue). An ellipse is fitted around the thresholded body pixels, and its main axis is used to measure the distribution of body pixels within 4 virtual quadrants whose origin is the centroid of the fly. The head region can be determined because it appears smaller in the camera images than the abdominal region of the fly.

Supplemental figure S10:

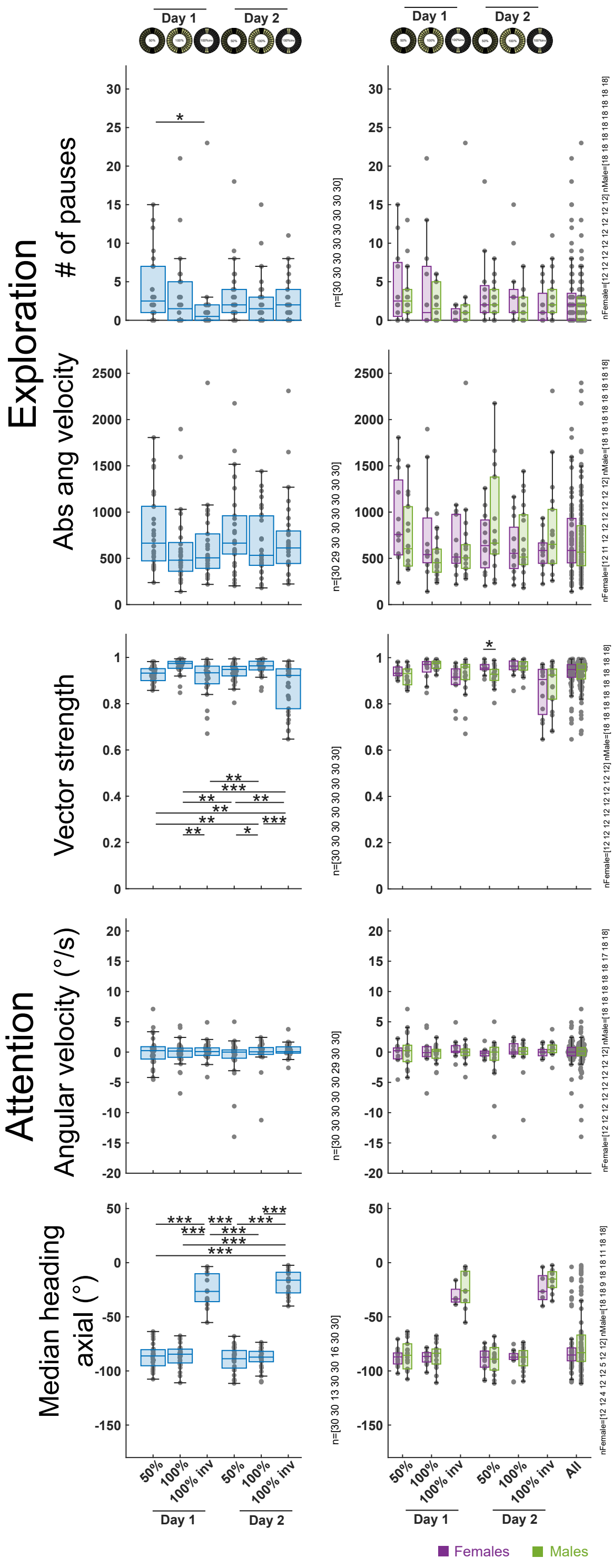

Supplemental figure S10: Population responses over time and different visual contrasts in flying flies. Boxplots illustrating key behavioral parameters for the whole population (blue) and separately for females/males (green/magenta) over time and varying stripe contrasts (**b**). Animal numbers are indicated next to each plot.

Supplemental figure S11:

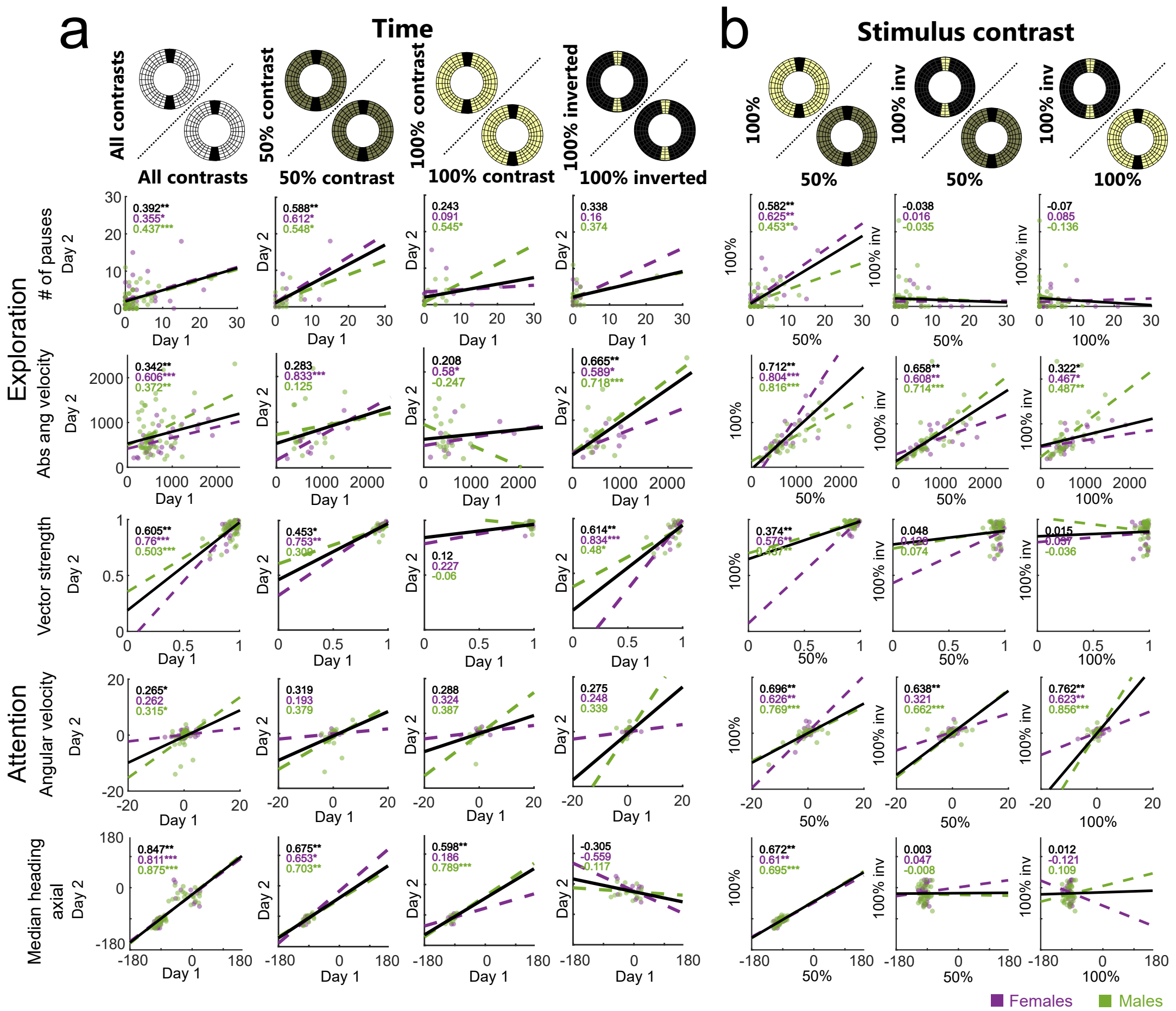

Supplemental Fig. S11: Sex-specific differences of individual traits in flying flies persist over time but depend on the visual scenery. **a** Correlation of key behavioral parameters for females and males over time and dependent on stimulus contrast. Magenta=females, green=males. Correlation coefficients are displayed in the upper left corner of each plot. *=$p<0.05$, **=$p<0.001$, ***=$p<0.0001$, for detailed fly numbers per experimental condition, see supplemental Fig. S10.

Supplemental figure S12:

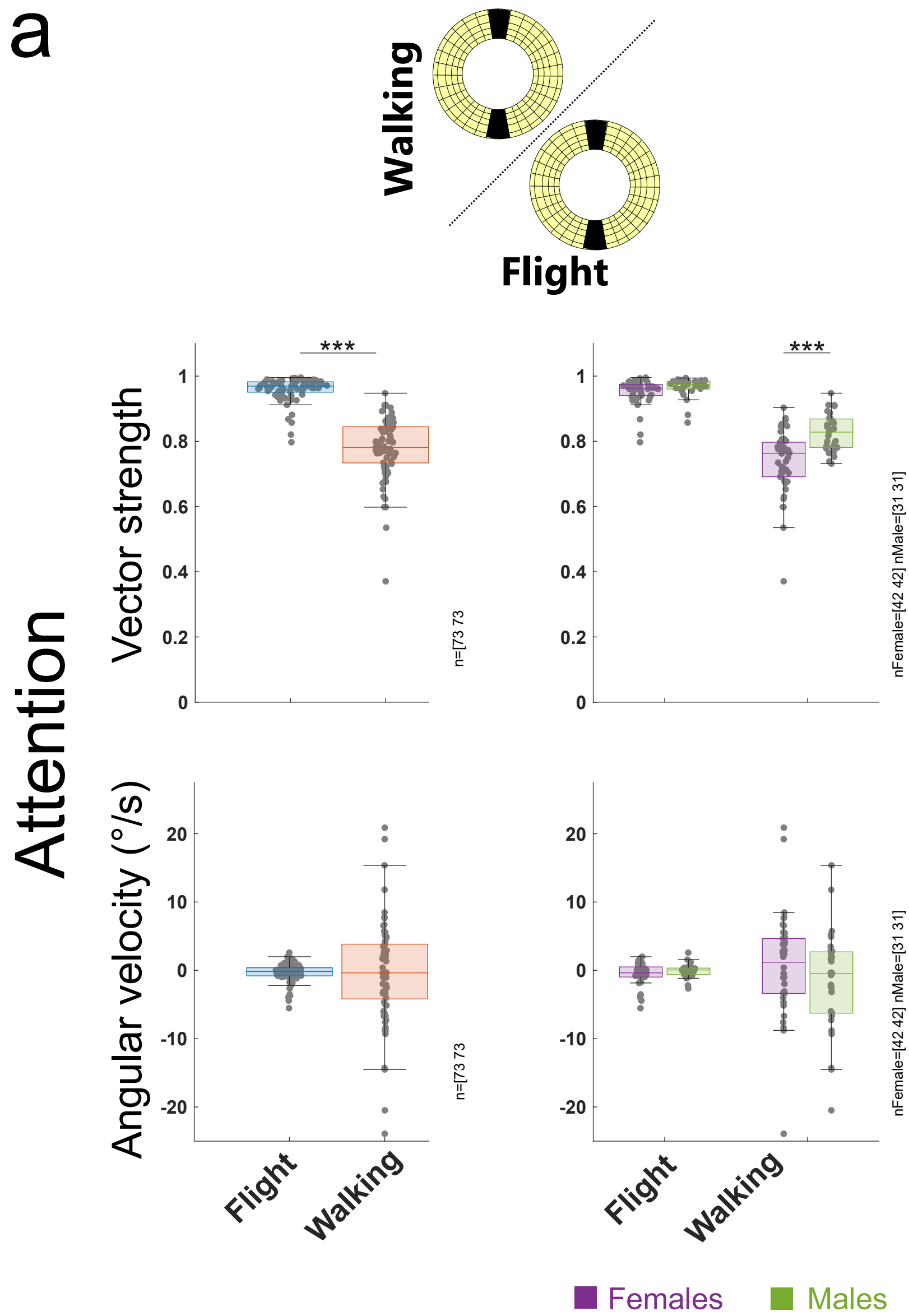

Supplemental Fig. S12: Population responses of orientational parameters across different behavioral states. Boxplots illustrating orientational parameters under different behavioral states for the whole test population (blue) and separately for females/males (green/magenta). Animal numbers are indicated next to each plot.

Supplemental figure S13:

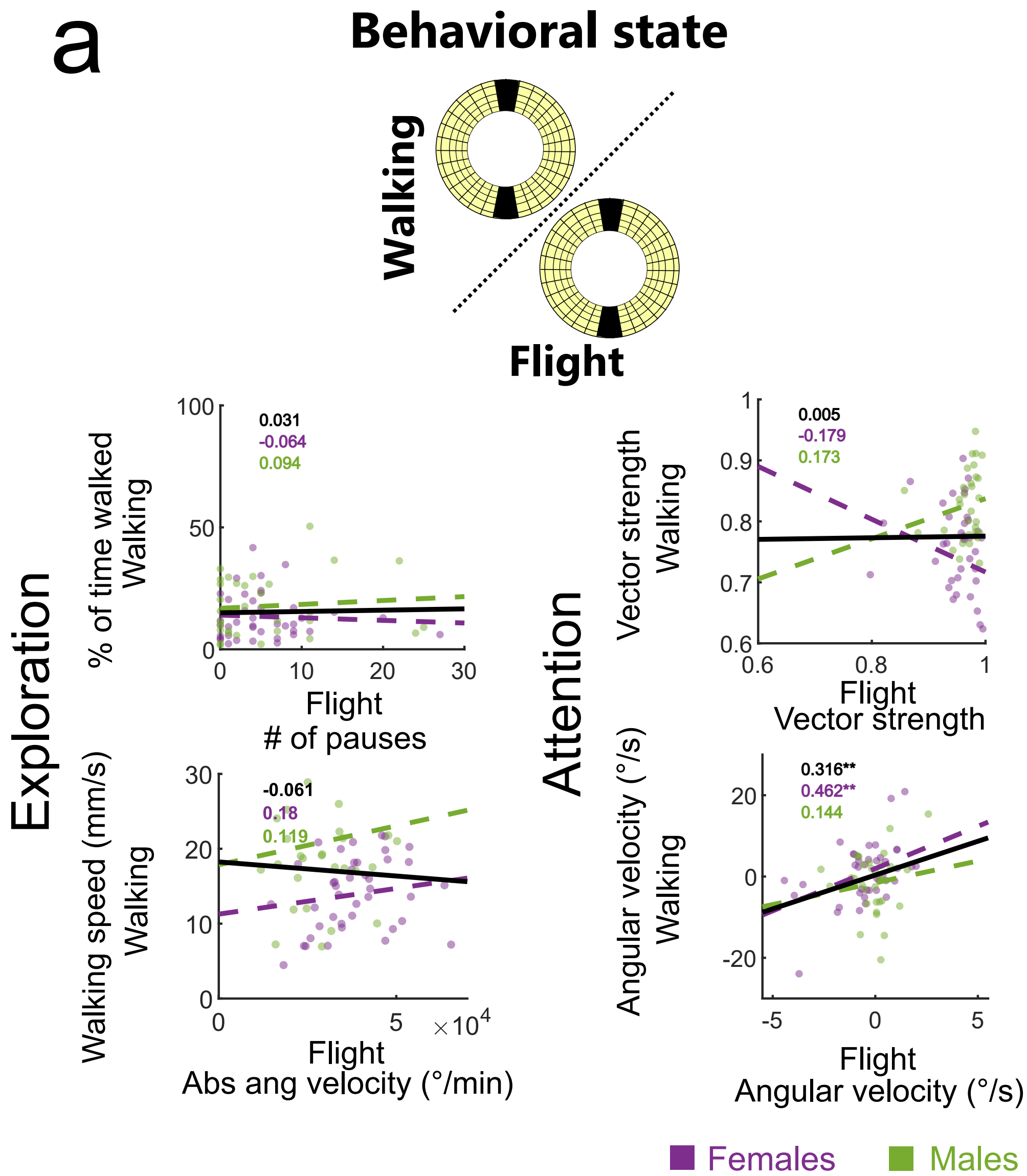

Supplemental Fig. S13: Attention persists across different behavioral states in males but not females. **a** Correlation of key behavioral parameters for females and males depending on the behavioral state. Magenta=females, green=males. Correlation coefficients are displayed in the upper left corner of each plot. *=p<0.05, **=p<0.001, ***=p<0.0001, for detailed fly numbers per experimental condition, see supplemental Fig. S12.

Supplemental table T1: Description of automatically computed output parameters

Parameter	Description
roinr	Arena number for fly identification.
sex	Male = 0, female = 1.
eucldistsum	Total distance walked in mm.
perctimemoving	% of time spent walking.
numberpauses	Number of pauses (min pause length = 1s).
medianpausedurati onsec	Median pause duration in s.
meanspeedmov	Mean walking speed in mm/s.
medianangleccenter moving	Median walking angle (heading direction) between 0° and 360° in the center region of the arena as seen from the animal.
medianangleccenter axialmoving	Median walking angle (heading direction) between 0° and 180° (axial) in the center region of the arena as seen from the animal. Axial transformation of angular data was achieved by subtracting 180 ° from all angles larger than 180 °. Axial data is more robust against cancelling -out of opposing angles in median calculations, e.g. when a fly is walking back and forth between stripes.
stddeviation	Standard deviation of angular data in ° as seen from the animal. Low angular standard deviation indicates a smaller range of chosen heading directions. Contains only data points where the animal was walking in the center region of the arena.
rlength	Resulting vector length of angular data mapped between 0° and 360°. A vector length of 0 would indicate uniform distribution of heading angles. A vector length of 1 would indicate the animl was only moving in a perfectly straight path. Contains only data points where the animal was walking in the center region of the arena.
rlengthax	Resulting vector length of angular data mapped between between 0° and 180° (axial) . A vector length of 0 would indicate uniform distribution of heading angles. A vector length of 1 would indicate the animl was only moving in a perfectly straight path. Contains only dat a points where the animal was walking in the center region of the arena. Axial data is more robust against cancelling -out of opposing angles in median calculations, e.g. when a fly is walking back and forth between stripes.
medianangvelmova lldegs	Median angular velocity (angular speed of azimuthal rotation) when walking in °/s. Median angular velocity is also a measure of handedness. Positive values indiceate right turns and negative values indicate left turns as seen from the animal.
medianangvelmovc enterdegs	Median angular velocity (angular speed of azimuthal rotation) when walking in the center region of the arena in °/s. Median angular velocity is also a measure of handedness. Positive values indiceate right turns and negative values indicate left turns as seen from the animal.
medianangvelmovo uterdegs	Median angular velocity (angular speed of azimuthal rotation) when walking in the edge region of the arena in °/s. Median angular velocity is also a measure of handedness. Positive values indiceate right turns and negative values indicate left turns as seen from the animal.
absturninganglesu m	Sum of all walking heading changes in °. Divided by distance walked this can be used as a measure for „meandering“ (heading change per mm walked in °/mm).
absturninganglesu mcenter	Sum of all walking heading changes within the center region of the arena in °. Divided by distance walked this can be used as a measure for „meandering“ (heading change per mm walked in °/mm).
centrophobindex	Centrophobicity index between 0 and 1. 0 indicates an animal being in the center area 100% of the time. 1 indicates an animal being in the edge area 100% of the time.
pecflymorethanone	% of time with more than two objects detected per arena. This parameter indicates false animal detections (e.g dust) and and is useful for validating tracking quality or finding tracking errors.
percflylost	% of time the tracker lost an animal. This parameter is useful for validating tracking quality or finding tracking errors.
stripedeviationmed ian	Applies to Buridan data. Medain angular distance to the closest (in terms of azimuthal rotation) stripe when walking in the center of the arena in °.
turnsnumber	Applies to Y -maze data. Number of turns. One turn is defined as an animal (measured at center point) walking from one Y-maze arm 3mm into another.
turnsbias	Ratio of right VS left turns. Values larger than 0.5 indicate right -handedness. Values smaller than 0.5 indicate left-handedness.

Supplemental table T2: Part list for setup replication

LED Buridan Setup		
Nr	**Description**	**Amount**
1	Flir Firefly S FFY-U3-04S2M-C + Edmund optics UC Series Fixed Focal Length Objective (8mm, Stock #33-307)	1
2	Acrylic plate white opaque matt 500 x 410 x 3 mm (30mm circular hole in center)	1
3	Clear acrylic cylinder (300mm diameter, 300mm height) + diffuser paper or satinice acrylic cylinder (300mm diameter, 300mm height)	1
4	Fluorscent tubes (Osram, L 40w, 640C circular cool white) + Osram QT-M 1626–42 controller for AC flicker rate >1kHz	4
5	Aluminium profiles black (45 x 45 mm) P45N10LS www.aluprofile24.de:	
	400mm + thread M12 (min 100mm) profile	4
	480mm profile	2
	485mm profile	1
	+ Construction accessories www.aluprofile24.de:	
	Wi45x45 angle	10
	IWiN10 angle	20
	BuMuM8 nut screw	20
	FußD40DG m12x100 feet	4
	+ BitFenix Spectre PRO 230 mm mounted between aluminium rails on 2 opposing sides of the setup for cooling the LED matrix	8
6	6x RGB LED matrix (128 x 64 pixel) www.ledall.de 1x Hdmi controller Novastar mctrl 660 pro + 1x Novastar A8S receiving card 6x	1
	+ Famotec locating ring 3mm inner diameter (EAN: 4053199955619) + grub screw M3 x 20mm for fixing LED matrix to the LED cylinder	150
7	Transparent acrylic dome 120mm diameter (www.architekturbedarf.de) coated with Sigmacote on the inside	1
8	PLEXIGLAS® WH10 DC white snow satinice disk 119 x 119 x 10 mm + 850nm LED strip wrapped around edge for backlight illumintaion	1
9	Acrylic plate white opaque matt 500 x 500 x 3 mm (120mm circular hole in center)	1
10	PLEXIGLAS® WH10 DC white snow satinice 500 x 500 x 3 mm	1
11	PLEXIGLAS® WH10 DC white snow satinice disk 119 x 119 x 10 mm + 850nm LED strip (www.ledxess.de) wrapped around edge for backlight illumintaion	1
12	PLEXIGLAS® WH10 DC white snow satinice 500 x 500 x 10 mm (300mm circular hole in center)	2
IndyTrax Setup		
Nr	**Description**	**Amount**
13	120x12mm EEC0381B1-000U-A99 Sunon	4
14	880nm infrared backlight https://www.amazon.de/LED-Lichttherapie-Dunkelrotes-Infrarot-LED-Lichttherapie-Panel-Hautverj%C3%BCngung-Druckentlastung/dp/B07ZQ	1
15	Server cabinet https://www.serverschrank24.de/15-he-serverschrank-wandgehause-mit-glastur-bxtxh-600-x-450-x-820-mm.html	1
16	Translucent acrylic cylinder https://www.kus-kunststofftechnik.de/plexiglas-rohr/plexiglasxt-satiniert-o-60-mm-laenge-waehlbar-von-100-bis-1400-mm/	25
16	Electroluminescent foil A7 white	50
16	Transparent dome 50mm https://www.dekoweltcreativ.de/acrylkugel-transparent-teilbar-stueck/p-3330.html	25
16	Plexiglas GS white 70% 3mm WH10 49mm diameter https://www.plattenzuschnitt24.de/Plexiglas-GS-weiss-WH10-GT-3mm.html	50
17	19" drawer https://www.it-budget.de/19-Fachboden-ausziehbar-Vollauszug-Tragkraft-30-kg-350-mm-schwarz	2
18	Camera Point Grey BFLY-PGE-23S6C-C mounted on Rack chassis 24563-194nVent – Schroff	1
18	Objective LM8HC3HOLE 1" 8mm/F1.4	1
19	BitFenix Spectre PRO 230 mm	2
20	Carbon heater https://thermowelt.de/Artikel/carbonheater1-1GN-220V.html	1
Controllers	Humidity controller TXG top-messtechnik.com TMT-HC-210 controlls 40x40mm Sunon EE40101S1-1000U-999 Axiallüfter 12 V/DC placed on (4)	1
	PID temperature controller pohltechnic.com RT4-121-Tr21Sd controlls (20)	1
	VOLTCRAFT LSP-1165 for controlling IR LED panel (14) and fans (18, 19)	2
	TT COMMANDER FT for cooling down enclosure, if necessary (controlls enclosure fans (13))	1
	Inverter https://www.el-light.shop/epages/17778431.sf/de_DE/?ObjectPath=/Shops/17778431/Products/InF1S150 controlls el-foil (16) brightness	1
LED flight simulator		
Nr	**Description**	**Amount**
21	Aluminium profiles black (30 x 30 mm) P30N8 www.aluprofile24.de:	
	600mm profile	4
	165mm profile	10
	200mm profile	2
	+ Construction accessories www.aluprofile24.de:	
	PADK30N8B cap	4
	IWIN8B angle	25
	BuMuM6 nut screw	10
	WI30N8B	10
	HaKoM6 (12mm)	20
22	optional servo motor for dorsal stimulus presentation (Dynamixel MX-12W) + ball bearing 6811-ZZ (www.kugellager-express.de)	1
23	4x RGB LED matrix (128 x 64 pixel) www.ledall.de + 1x Hdmi controller Novastar mctrl 660 pro + 1x Novastar A8S receiving card	1
	+ Famotec locating ring 3mm inner diameter (EAN: 4053199955619) + grub screw M3 x 20mm for fixing LED matrix to the LED cylinder	150
24	Neodynium cylinder magnet (5mm diameter, 20mm height) + white plastic cap + 1mm diameter v-shaped sapphire bearing in center for friction reduction	1
25	Neodynium ring magnet (10mm diameter, 5mm height, inner diameter 5mm) + white plastic cap	1
26	850nm near infrared LED array (https://www.amazon.de/POFET-Infrarot-IR-LED-850-nm-Platinenmodul-f%C3%BCr-das-Kamera%C3%Bcberwachungssystem)	1
27	Flir Firefly S FFY-U3-04S2M-C + Edmund optics UC Series Fixed Focal Length Objective (12mm, Stock #33-307)	1
Air puffs	Arduino UNO Rev3 + relais module + Schego membrane pump 300l/h	1

References

1. Gosling, S.D. (2008). Personality in Non-human Animals. Social and Personality Psychology Compass *2*, 985-1001. https://doi.org/10.1111/j.1751-9004.2008.00087.x.
2. Dall, S.R.X., Houston, A.I., and McNamara, J.M. (2004). The behavioural ecology of personality: consistent individual differences from an adaptive perspective. Ecology Letters *7*, 734-739. https://doi.org/10.1111/j.1461-0248.2004.00618.x.
3. Reale, D., Reader, S.M., Sol, D., McDougall, P.T., and Dingemanse, N.J. (2007). Integrating animal temperament within ecology and evolution. Biol Rev Camb Philos Soc *82*, 291-318. 10.1111/j.1469-185X.2007.00010.x.
4. Andrew Sih, Alison M Bell, J Chadwick Johnson, and Robert E Ziemba (2004). Behavioral Syndromes: An Integrative Overview. The Quarterly Review of Biology *79*, 241-277. 10.1086/422893.
5. Freund, J., Brandmaier, A.M., Lewejohann, L., Kirste, I., Kritzler, M., Krüger, A., Sachser, N., Lindenberger, U., and Kempermann, G. (2013). Emergence of Individuality in Genetically Identical Mice. Science *340*, 756-759. doi:10.1126/science.1235294.
6. Partridge, L. (1976). Individual differences in feeding efficiencies and feeding preferences of captive great tits. Animal Behaviour *24*, 230-240. https://doi.org/10.1016/S0003-3472(76)80119-4.
7. Mather, J., and Anderson, R.C. (1993). Personalities of octopuses (Octopus rubescens). Journal of Comparative Psychology *107*, 336-340.
8. Schuett, W., Dall, S.R.X., Baeumer, J., Kloesener, M.H., Nakagawa, S., Beinlich, F., and Eggers, T. (2011). Personality variation in a clonal insect: The pea aphid, Acyrthosiphon pisum. Developmental Psychobiology *53*, 631-640. https://doi.org/10.1002/dev.20538.
9. Ayroles, J.F., Buchanan, S.M., O'Leary, C., Skutt-Kakaria, K., Grenier, J.K., Clark, A.G., Hartl, D.L., and de Bivort, B.L. (2015). Behavioral idiosyncrasy reveals genetic control of phenotypic variability. Proceedings of the National Academy of Sciences *112*, 6706-6711. doi:10.1073/pnas.1503830112.
10. Buchanan, S.M., Kain, J.S., and de Bivort, B.L. (2015). Neuronal control of locomotor handedness in Drosophila. Proc Natl Acad Sci U S A *112*, 6700-6705. 10.1073/pnas.1500804112.
11. Honegger, K.S., Smith, M.A.-Y., Churgin, M.A., Turner, G.C., and de Bivort, B.L. (2020). Idiosyncratic neural coding and neuromodulation of olfactory individuality in Drosophila. Proceedings of the National Academy of Sciences *117*, 23292-23297. doi:10.1073/pnas.1901623116.
12. Kain, J.S., Stokes, C., and de Bivort, B.L. (2012). Phototactic personality in fruit flies and its suppression by serotonin and white. Proceedings of the National Academy of Sciences *109*, 19834-19839. doi:10.1073/pnas.1211988109.
13. Linneweber, G.A., Andriatsilavo, M., Dutta, S.B., Bengochea, M., Hellbruegge, L., Liu, G., Ejsmont, R.K., Straw, A.D., Wernet, M., Hiesinger, P.R., and Hassan, B.A. (2020). A neurodevelopmental origin of behavioral individuality in the Drosophila visual system. Science *367*, 1112-1119. 10.1126/science.aaw7182.
14. Kahsai, L., and Zars, T. (2011). Learning and Memory in Drosophila: Behavior, Genetics, and Neural Systems. In International Review of Neurobiology, N. Atkinson, ed. (Academic Press), pp. 139-167. https://doi.org/10.1016/B978-0-12-387003-2.00006-9.
15. Lapiedra, O., Schoener, T.W., Leal, M., Losos, J.B., and Kolbe, J.J. (2018). Predator-driven natural selection on risk-taking behavior in anole lizards. Science *360*, 1017-1020. doi:10.1126/science.aap9289.
16. Galton, F. (1875). The history of twins, as a criterion of the relative powers of nature and nurture. Fraser's Magazine *12*, 566-576.

17. Honegger, K., and de Bivort, B. (2018). Stochasticity, individuality and behavior. Curr Biol *28*, R8-R12. 10.1016/j.cub.2017.11.058.
18. Traynor, B.J., and Singleton, A.B. (2010). Nature versus Nurture: Death of a Dogma, and the Road Ahead. Neuron *68*, 196-200. https://doi.org/10.1016/j.neuron.2010.10.002.
19. Mischel, W. (1968). Personality and assessment (Wiley).
20. Takola, E., and Schielzeth, H. (2022). Hutchinson's ecological niche for individuals. Biology & Philosophy *37*, 25. 10.1007/s10539-022-09849-y.
21. Briffa, M., Rundle, S.D., and Fryer, A. (2008). Comparing the strength of behavioural plasticity and consistency across situations: animal personalities in the hermit crab Pagurus bernhardus. Proc Biol Sci *275*, 1305-1311. 10.1098/rspb.2008.0025.
22. Mowles, S.L., Cotton, P.A., and Briffa, M. (2012). Consistent crustaceans: the identification of stable behavioural syndromes in hermit crabs. Behavioral Ecology and Sociobiology *66*, 1087-1094. 10.1007/s00265-012-1359-7.
23. Herborn, K.A., Macleod, R., Miles, W.T.S., Schofield, A.N.B., Alexander, L., and Arnold, K.E. (2010). Personality in captivity reflects personality in the wild. Animal Behaviour *79*, 835-843. 10.1016/j.anbehav.2009.12.026.
24. Kralj-Fišer, S., Scheiber, I.B.R., Blejec, A., Moestl, E., and Kotrschal, K. (2007). Individualities in a flock of free-roaming greylag geese: Behavioral and physiological consistency over time and across situations. Hormones and Behavior *51*, 239-248. https://doi.org/10.1016/j.yhbeh.2006.10.006.
25. Coleman, K., and Wilson, D.S. (1998). Shyness and boldness in pumpkinseed sunfish: individual differences are context-specific. Animal Behaviour *56*, 927-936. https://doi.org/10.1006/anbe.1998.0852.
26. D'Eath, R., and Burn, C. (2002). INDIVIDUAL DIFFERENCES IN BEHAVIOUR: A TEST OF 'COPING STYLE' DOES NOT PREDICT RESIDENT-INTRUDER AGGRESSIVENESS IN PIGS. Behaviour *139*, 1175-1194. https://doi.org/10.1163/15685390260437326.
27. Werkhoven, Z., Bravin, A., Skutt-Kakaria, K., Reimers, P., Pallares, L.F., Ayroles, J., and de Bivort, B.L. (2021). The structure of behavioral variation within a genotype. eLife *10*, e64988. 10.7554/eLife.64988.
28. Boissy, A., and Bouissou, M.F. (1995). Assessment of individual differences in behavioural reactions of heifers exposed to various fear-eliciting situations. Applied Animal Behaviour Science *46*, 17-31. https://doi.org/10.1016/0168-1591(95)00633-8.
29. Spoolder, H.A.M., Burbidge, J.A., Lawrence, A.B., Simmins, P.H., and Edwards, S.A. (1996). Individual behavioural differences in pigs: Intra- and inter-test consistency. Applied Animal Behaviour Science *49*, 185-198. 10.1016/0168-1591(96)01033-7.
30. Costa, P.T., Jr., and McCrae, R.R. (1988). Personality in adulthood: a six-year longitudinal study of self-reports and spouse ratings on the NEO Personality Inventory. J Pers Soc Psychol *54*, 853-863. 10.1037//0022-3514.54.5.853.
31. Weisbuch, M., Slepian, M.L., Clarke, A., Ambady, N., and Veenstra-Vanderweele, J. (2010). Behavioral Stability Across Time and Situations: Nonverbal Versus Verbal Consistency. J Nonverbal Behav *34*, 43. 10.1007/s10919-009-0079-9.
32. Ross, L. (1977). The Intuitive Psychologist And His Shortcomings: Distortions in the Attribution Process11The author gratefully acknowledges the assistance of Teresa Amabile, Daryl Bern, Phoebe Ellsworth, Baruch Fischhoff, David Greene, Larry Gross, Mark Lepper, Richard Nisbett, Julia Steinmetz, Amos Tversky, and Philip Zimbardo, all of whom have contributed useful comments and suggestions concerning both the manuscript and the research and conceptual analysis it reports. The preparation of this chapter and reported research were supported by National Institute of Mental Health Research Grant MH 24134. In Advances in Experimental Social Psychology, L. Berkowitz, ed. (Academic Press), pp. 173-220. https://doi.org/10.1016/S0065-2601(08)60357-3.
33. Fleeson, W. (2001). Toward a structure- and process-integrated view of personality: traits as density distribution of states. J Pers Soc Psychol *80*, 1011-1027.

34. Hartshorne, H., and May, M.A. (1930). Studies in the Nature of Character: Studies in deceit (McMillian).
35. Xu, C.S., Januszewski, M., Lu, Z., Takemura, S.-y., Hayworth, K.J., Huang, G., Shinomiya, K., Maitin-Shepard, J., Ackerman, D., Berg, S., et al. (2020). A Connectome of the Adult Drosophila Central Brain. bioRxiv, 2020.2001.2021.911859. 10.1101/2020.01.21.911859.
36. Zheng, Z., Lauritzen, J.S., Perlman, E., Robinson, C.G., Nichols, M., Milkie, D., Torrens, O., Price, J., Fisher, C.B., Sharifi, N., et al. (2018). A Complete Electron Microscopy Volume of the Brain of Adult Drosophila melanogaster. Cell *174*, 730-743 e722. 10.1016/j.cell.2018.06.019.
37. Luan, H., Peabody, N.C., Vinson, C.R., and White, B.H. (2006). Refined spatial manipulation of neuronal function by combinatorial restriction of transgene expression. Neuron *52*, 425-436. 10.1016/j.neuron.2006.08.028.
38. Pfeiffer, B.D., Ngo, T.T., Hibbard, K.L., Murphy, C., Jenett, A., Truman, J.W., and Rubin, G.M. (2010). Refinement of tools for targeted gene expression in Drosophila. Genetics *186*, 735-755. 10.1534/genetics.110.119917.
39. Baines, R.A., Uhler, J.P., Thompson, A., Sweeney, S.T., and Bate, M. (2001). Altered Electrical Properties in DrosophilaNeurons Developing without Synaptic Transmission. The Journal of Neuroscience *21*, 1523-1531. 10.1523/jneurosci.21-05-01523.2001.
40. Sweeney, S.T., Broadie, K., Keane, J., Niemann, H., and O'Kane, C.J. (1995). Targeted expression of tetanus toxin light chain in Drosophila specifically eliminates synaptic transmission and causes behavioral defects. Neuron *14*, 341-351. 10.1016/0896-6273(95)90290-2.
41. Luan, H., Lemon, W.C., Peabody, N.C., Pohl, J.B., Zelensky, P.K., Wang, D., Nitabach, M.N., Holmes, T.C., and White, B.H. (2006). Functional dissection of a neuronal network required for cuticle tanning and wing expansion in Drosophila. J Neurosci *26*, 573-584. 10.1523/JNEUROSCI.3916-05.2006.
42. Hamada, F.N., Rosenzweig, M., Kang, K., Pulver, S.R., Ghezzi, A., Jegla, T.J., and Garrity, P.A. (2008). An internal thermal sensor controlling temperature preference in Drosophila. Nature *454*, 217-220. 10.1038/nature07001.
43. Pulver, S.R., Pashkovski, S.L., Hornstein, N.J., Garrity, P.A., and Griffith, L.C. (2009). Temporal dynamics of neuronal activation by Channelrhodopsin-2 and TRPA1 determine behavioral output in Drosophila larvae. J Neurophysiol *101*, 3075-3088. 10.1152/jn.00071.2009.
44. Klapoetke, N.C., Murata, Y., Kim, S.S., Pulver, S.R., Birdsey-Benson, A., Cho, Y.K., Morimoto, T.K., Chuong, A.S., Carpenter, E.J., Tian, Z., et al. (2014). Independent optical excitation of distinct neural populations. Nat Methods *11*, 338-346. 10.1038/nmeth.2836.
45. Bülthoff, H., Götz, K.G., and Herre, M. (1982). Recurrent inversion of visual orientation in the walking fly,Drosophila melanogaster. Journal of comparative physiology *148*, 471-481. 10.1007/BF00619785.
46. Götz, K.G. (1980). Visual Guidance in Drosophila. In Development and Neurobiology of Drosophila, O. Siddiqi, P. Babu, L.M. Hall, and J.C. Hall, eds. (Springer US), pp. 391-407. 10.1007/978-1-4684-7968-3_28.
47. Seelig, J.D., Chiappe, M.E., Lott, G.K., Dutta, A., Osborne, J.E., Reiser, M.B., and Jayaraman, V. (2010). Two-photon calcium imaging from head-fixed Drosophila during optomotor walking behavior. Nat Methods *7*, 535-540. 10.1038/nmeth.1468.
48. Mathejczyk, T.F., and Wernet, M.F. (2020). Modular assays for the quantitative study of visually guided navigation in both flying and walking flies. Journal of Neuroscience Methods *340*, 108747. https://doi.org/10.1016/j.jneumeth.2020.108747.
49. Mathejczyk, T.F., and Wernet, M.F. (2019). Heading choices of flying Drosophila under changing angles of polarized light. Sci Rep *9*, 16773. 10.1038/s41598-019-53330-y.
50. Hassan, B.A., Bermingham, N.A., He, Y., Sun, Y., Jan, Y.N., Zoghbi, H.Y., and Bellen, H.J. (2000). atonal regulates neurite arborization but does not act as a proneural gene in the Drosophila brain. Neuron *25*, 549-561. 10.1016/s0896-6273(00)81059-4.

51. Otsuna, H., and Ito, K. (2006). Systematic analysis of the visual projection neurons of Drosophila melanogaster. I. Lobula-specific pathways. J Comp Neurol *497*, 928-958. 10.1002/cne.21015.
52. Strauss, R., Hanesch, U., Kinkelin, M., Wolf, R., and Heisenberg, M. (1992). No-Bridge of Drosophila Melanogaster: Portrait of a Structural Brain Mutant of the Central Complex. Journal of Neurogenetics *8*, 125-155. 10.3109/01677069209083444.
53. Kiral, F.R., Linneweber, G.A., Mathejczyk, T., Georgiev, S.V., Wernet, M.F., Hassan, B.A., von Kleist, M., and Hiesinger, P.R. (2020). Autophagy-dependent filopodial kinetics restrict synaptic partner choice during Drosophila brain wiring. Nature Communications *11*, 1325. 10.1038/s41467-020-14781-4.
54. Strauss, R., Renner, M., and Götz, K. (2001). Task-specific association of photoreceptor systems and steering parameters in Drosophila. Journal of Comparative Physiology A *187*, 617-632. 10.1007/s003590100234.
55. Neuser, K., Triphan, T., Mronz, M., Poeck, B., and Strauss, R. (2008). Analysis of a spatial orientation memory in Drosophila. Nature *453*, 1244-1247. 10.1038/nature07003.
56. Valente, D., Golani, I., and Mitra, P.P. (2007). Analysis of the trajectory of Drosophila melanogaster in a circular open field arena. PLoS One *2*, e1083. 10.1371/journal.pone.0001083.
57. Branson, K., Robie, A.A., Bender, J., Perona, P., and Dickinson, M.H. (2009). High-throughput ethomics in large groups of Drosophila. Nat Methods *6*, 451-457. 10.1038/nmeth.1328.
58. Robie, A.A., Hirokawa, J., Edwards, A.W., Umayam, L.A., Lee, A., Phillips, M.L., Card, G.M., Korff, W., Rubin, G.M., Simpson, J.H., et al. (2017). Mapping the Neural Substrates of Behavior. Cell *170*, 393-406 e328. 10.1016/j.cell.2017.06.032.
59. Hirsch, J., and Boudreau, J.C. (1958). Studies in experimental behavior genetics. I. The heritability of phototaxis in a population of Drosophila melanogaster. J Comp Physiol Psychol *51*, 647-651. 10.1037/h0039498.
60. Hirsch, J. (1959). Studies in experimental behavior genetics. II. Individual differences in geotaxis as a function of chromosome variations in synthesized Drosophila populations. J Comp Physiol Psychol *52*, 304-308. 10.1037/h0043498.
61. Quinn, W.G., Harris, W.A., and Benzer, S. (1974). Conditioned Behavior in Drosophila melanogaster. Proceedings of the National Academy of Sciences *71*, 708-712. 10.1073/pnas.71.3.708.
62. Jiang, H., Hanna, E., Gatto, C.L., Page, T.L., Bhuva, B., and Broadie, K. (2016). A fully automated Drosophila olfactory classical conditioning and testing system for behavioral learning and memory assessment. Journal of Neuroscience Methods *261*, 62-74. https://doi.org/10.1016/j.jneumeth.2015.11.030.
63. Konopka, R.J., and Benzer, S. (1971). Clock Mutants of Drosophila melanogaster. Proceedings of the National Academy of Sciences *68*, 2112-2116. 10.1073/pnas.68.9.2112.
64. Geissmann, Q., Garcia Rodriguez, L., Beckwith, E.J., French, A.S., Jamasb, A.R., and Gilestro, G.F. (2017). Ethoscopes: An open platform for high-throughput ethomics. PLOS Biology *15*, e2003026. 10.1371/journal.pbio.2003026.
65. Werkhoven, Z., Rohrsen, C., Qin, C., Brembs, B., and de Bivort, B. (2019). MARGO (Massively Automated Real-time GUI for Object-tracking), a platform for high-throughput ethology. PLoS One *14*, e0224243. 10.1371/journal.pone.0224243.
66. Warren, T.L., Weir, P.T., and Dickinson, M.H. (2018). Flying Drosophila melanogaster maintain arbitrary but stable headings relative to the angle of polarized light. Journal of Experimental Biology *221*. 10.1242/jeb.177550.
67. Colomb, J., Reiter, L., Blaszkiewicz, J., Wessnitzer, J., and Brembs, B. (2012). Open source tracking and analysis of adult Drosophila locomotion in Buridan's paradigm with and without visual targets. PLoS One *7*, e42247. 10.1371/journal.pone.0042247.
68. Berens, P. (2009). CircStat: A MATLAB Toolbox for Circular Statistics. 2009 *31*, 21. 10.18637/jss.v031.i10.

69. Gibert, J.P., Chelini, M.-C., Rosenthal, M.F., and DeLong, J.P. (2016). Crossing regimes of temperature dependence in animal movement. Global Change Biology *22*, 1722-1736. https://doi.org/10.1111/gcb.13245.
70. Han, R., Wei, T.-M., Tseng, S.-C., and Lo, C.-C. (2021). Characterizing approach behavior of Drosophila melanogaster in Buridan's paradigm. PLOS ONE *16*, e0245990. 10.1371/journal.pone.0245990.
71. Vansteelandt, K., and Van Mechelen, I. (2004). The personality triad in balance: Multidimensional individual differences in situation–behavior profiles. Journal of Research in Personality *38*, 367-393. https://doi.org/10.1016/j.jrp.2003.08.001.
72. Bell, A.M., Hankison, S.J., and Laskowski, K.L. (2009). The repeatability of behaviour: a meta-analysis. Animal Behaviour *77*, 771-783. https://doi.org/10.1016/j.anbehav.2008.12.022.
73. Briffa, M., and Greenaway, J. (2011). High In Situ Repeatability of Behaviour Indicates Animal Personality in the Beadlet Anemone Actinia equina (Cnidaria). PLOS ONE *6*, e21963. 10.1371/journal.pone.0021963.
74. Diener, E., and Larsen, R.J. (1984). Temporal stability and cross-situational consistency of affective, behavioral, and cognitive responses. J Pers Soc Psychol *47*, 871-883. 10.1037//0022-3514.47.4.871.
75. Versace, E., Caffini, M., Werkhoven, Z., and de Bivort, B.L. (2020). Individual, but not population asymmetries, are modulated by social environment and genotype in Drosophila melanogaster. Scientific Reports *10*, 4480. 10.1038/s41598-020-61410-7.
76. Mischel, W., and Shoda, Y. (1995). A cognitive-affective system theory of personality: reconceptualizing situations, dispositions, dynamics, and invariance in personality structure. Psychol Rev *102*, 246-268. 10.1037/0033-295x.102.2.246.
77. Mischel, W., and Shoda, Y. (1998). RECONCILING PROCESSING DYNAMICS AND PERSONALITY DISPOSITIONS. Annual Review of Psychology *49*, 229-258. 10.1146/annurev.psych.49.1.229.
78. Sih, A., Cote, J., Evans, M., Fogarty, S., and Pruitt, J. (2012). Ecological implications of behavioural syndromes. Ecology Letters *15*, 278-289. https://doi.org/10.1111/j.1461-0248.2011.01731.x.
79. Pantoja, C., Hoagland, A., Carroll, E.C., Karalis, V., Conner, A., and Isacoff, E.Y. (2016). Neuromodulatory Regulation of Behavioral Individuality in Zebrafish. Neuron *91*, 587-601. 10.1016/j.neuron.2016.06.016.
80. Mischel, W. (1973). Toward a cognitive social learning reconceptualization of personality. Psychol Rev *80 4*, 252-283.
81. Lithgow, G.J., Driscoll, M., and Phillips, P. (2017). A long journey to reproducible results. Nature *548*, 387-388. 10.1038/548387a.
82. Crabbe, J.C., Wahlsten, D., and Dudek, B.C. (1999). Genetics of Mouse Behavior: Interactions with Laboratory Environment. Science *284*, 1670-1672. doi:10.1126/science.284.5420.1670.